TABLE 4. Comparison of Clinical Characteristics of Patients with Glaucoma, According to *OPTN* Genotypes

	Phenotype Variable	G/G	G/A + A/A	P*
c.412G→A (Thr34Thr)				
POAG	Age at diagnosis (y)	58.1 ± 11.8 (*n* = 123)	58.8 ± 12.6 (*n* = 69)	0.663
	IOP at diagnosis (mm Hg)	27.0 ± 6.5 (*n* = 112)	26.1 ± 5.0 (*n* = 60)	0.360
	Visual field score at diagnosis	3.0 ± 0.9 (*n* = 125)	3.2 ± 0.9 (*n* = 69)	0.093
NTG	Age at diagnosis (y)	58.7 ± 11.7 (*n* = 148)	56.6 ± 11.2 (*n* = 69)	0.206
	IOP at diagnosis (mm Hg)	16.4 ± 2.6 (*n* = 139)	16.6 ± 2.2 (*n* = 67)	0.848
	Visual field score at diagnosis	2.8 ± 0.7 (*n* = 148)	2.7 ± 0.7 (*n* = 69)	0.135
	Phenotype Variable	**T/T**	**T/A + A/A**	**P***
c.603T→A (Met98Lys)				
POAG	Age at diagnosis (y)	57.6 ± 11.9 (*n* = 159)	62.2 ± 12.4 (*n* = 33)	0.046†
	IOP at diagnosis (mm Hg)	26.8 ± 5.8 (*n* = 143)	26.5 ± 7.1 (*n* = 29)	0.931
	Visual field score at diagnosis	3.1 ± 0.9 (*n* = 161)	3.2 ± 0.9 (*n* = 33)	0.280
NTG	Age at diagnosis (y)	58.4 ± 11.6 (*n* = 169)	56.6 ± 11.6 (*n* = 48)	0.304
	IOP at diagnosis (mm Hg)	16.4 ± 2.4 (*n* = 160)	16.8 ± 2.6 (*n* = 46)	0.270
	Visual field score at diagnosis	2.8 ± 0.7 (*n* = 169)	2.8 ± 0.6 (*n* = 48)	0.318

* *P* by Mann-Whitney test.
† $P < 0.05$.

as a glaucoma-causing gene in Japanese patients with POAG or NTG.

Our observations showed that the frequency of the A allele in c.603T→A (Met98Lys) was slightly higher in patients with NTG (A: 12.2%, $P = 0.071$) than in patients with POAG (A: 8.8%) or control subjects (A: 8.5%). The Met98Lys change was observed as 22.1% in NTG ($P = 0.139$), 17.0% in POAG ($P = 0.893$), and 16.5% in control subjects. In the United Kingdom, a significant association of Met98Lys with NTG but not POAG has been reported.[19] These results suggest that there may be genetic differences between the two phenotypes. Tang et al.[16] reported no significant difference in allele frequency between Japanese patients with POAG or NTG and control subjects for Thr34Thr, Met98Lys, or Arg545Gln. In contrast, Alward et al.[20] observed a significantly higher prevalence ($P = 0.01$) of the Met98Lys change in 51 (20.7%) of 247 Japanese patients with NTG, compared with 8 (9.0%) of 89 Japanese control subjects. However, the number of control subjects in their study was too few to perform a case–control association study.

In patients with POAG in France and Morocco, the Met98Lys frequency was similar to that of control subjects.[39] However, a Met98Lys variant was reported to be significantly associated with a lower initial IOP: There was a downward shift of the initial IOP in patients with POAG harboring Met98Lys.[39] In our study, a Met98Lys variant was not associated with a lower initial IOP, but was weakly ($P = 0.046$) associated with an older age at diagnosis in patients with POAG.

No significant difference in the frequency of the Arg545Gln variant was found between Japanese patients with glaucoma and control subjects. In a Chinese population, the Met98Lys and Arg545Gln variants were reported to have similar frequencies in patients with glaucoma and control subjects.[18] Arg545Gln is a common polymorphism in the Japanese and Chinese populations, but may be rare in whites.[20]

The distribution of c.412G→A (Thr34Thr) genotype in the *OPTN* gene differed significantly between POAG ($P = 0.011$) and control subjects in our Japanese population, with the A allele being significantly more frequent than the G allele (POAG, $P = 0.003$). This polymorphism is associated with POAG more than NTG ($P = 0.078$ in genotype frequency and $P = 0.034$ in allele frequency). This finding is new, although the c.412G→A polymorphism has been identified in the United States,[13,20] Finland,[15] Hong Kong,[18] and Japan.[16,20] Previous studies of this polymorphism in Japanese patients did not find an association with glaucoma.[16,20] Our Japanese subjects resided throughout the nation and consisted of a larger number of subjects, which may account for the differing results.

Although the reason for the significant association of the c.412G→A polymorphism with patients with glaucoma is unknown, it may be linked to another unknown single-nucleotide polymorphism that exists in the promoter region and may alter the activity of the protein or may affect the stability or splicing accuracy of the mRNA.[40] Alternatively, the c.412G→A polymorphism may be linked to another unknown gene that lies near the *OPTN* gene.[41]

TABLE 5. Genotype Distribution of Three Polymorphisms of the 5′ Flanking Region of the TNF-α Gene in Patients with Glaucoma and Controls Subjects

		Genotype Frequency (%)			
Phenotype	***n***	**G/G**	**G/A**	**A/A**	***P****
−308G→A					
POAG	194	192 (99.0)	2 (1.0)	0 (0)	0.442
NTG	217	211 (97.2)	6 (2.8)	0 (0)	1
Control	218	212 (97.2)	6 (2.8)	0 (0)	
		Genotype Frequency (%)			
Phenotype	***n***	**C/C**	**C/T**	**T/T**	***P****
−857C→T					
POAG	194	135 (69.5)	49 (25.3)	10 (5.2)	0.138
NTG	217	148 (68.2)	64 (29.5)	5 (2.3)	0.890
Control	218	144 (66.1)	69 (31.6)	5 (2.3)	
		Genotype Frequency (%)			
Phenotype	***n***	**C/C**	**C/A**	**A/A**	***P****
−863C→A					
POAG	194	141 (72.7)	46 (23.7)	7 (3.6)	0.056
NTG	217	159 (73.3)	55 (25.3)	3 (1.4)	0.606
Control	218	161 (73.8)	56 (25.7)	1 (0.5)	

* *P* by χ^2 test.

TABLE 6. Distribution of Optineurin Genotypes (c.412G→A and c.603T→A) According to TNF-α Genotypes (−857C→T and −863C→A) in Glaucoma Patients and Control Subjects

Phenotype	−857C→T C/C(%)			Odds Ratio 95% CI	C/T + T/T (%)			Odds Ratio 95% CI
	c.412G→A	G/G	G/A + A/A	P*		G/G	G/A + A/A	P*
c.412G→A (Thr34Thr)								
POAG		92 (68.1)	43 (31.9)	0.204	1.40 (0.83–2.37)	33 (55.9)	26 (44.1)	0.006‡	2.86 (1.34–6.08)
NTG		97 (65.5)	51 (34.5)	0.077	1.58 (0.95–2.62)	51 (73.9)	18 (26.1)	0.531	1.28 (0.59–2.77)
Control		108 (75.0)	36 (25.0)			58 (78.4)	16 (21.6)		
	−863C→A C/C (%)					C/A + A/A (%)			
Phenotype	c.412G→A	G/G	G/A + A/A	P*	Odds Ratio 95% CI	G/G	G/A + A/A	P*	Odds Ratio 95% CI
POAG		91 (64.5)	50 (35.5)	0.017	1.84 (1.11–3.05)	34 (64.2)	19 (35.8)	0.280	1.56 (0.69–3.53)
NTG		110 (69.2)	49 (30.8)	0.114	1.49 (0.91–2.46)	38 (65.5)	20 (34.5)	0.341	1.47 (0.66–3.28)
Control		124 (77.0)	37 (23.0)			42 (73.7)	15 (26.3)		
	−857C→T C/C(%)					C/T + T/T (%)			
Phenotype	c.603T→A	T/T	T/A + A/A	P*	Odds Ratio 95% CI	T/T	T/A + A/A	P*	Odds Ratio 95% CI
c.603T→A (Met98Lys)									
POAG		112 (83.0)	23 (17.0)	0.811	1.08 (0.57–2.03)	49 (83.1)	10 (16.9)	0.925	0.96 (0.39–2.37)
NTG		111 (75.0)	37 (25.0)	0.056	1.75 (0.98–3.13)	58 (84.1)	11 (15.9)	0.795	0.89 (0.37–2.14)
Control		121 (84.0)	23 (16.0)			61 (82.4)	13 (17.6)		
	−863C→A C/C (%)					C/A + A/A (%)			
Phenotype	c.603T→A	T/T	T/A + A/A	P*	Odds Ratio 95% CI	T/T	T/A + A/A	P*	Odds Ratio 95% CI
POAG		123 (87.2)	18 (12.8)	0.127	0.61 (0.33–1.15)	38 (71.7)	15 (28.3)	0.008‡	4.11 (1.37–12.27)
NTG		125 (78.6)	34 (21.4)	0.636	1.14 (0.66–1.97)	44 (75.9)	14 (24.1)	0.027†	3.31 (1.10–9.91)
Control		130 (80.7)	31 (19.3)			52 (91.2)	5 (8.8)		

* P by χ^2 test.
† $P < 0.05$.
‡ $P < 0.01$.

Optineurin is induced by TNF-α and interacts with several proteins to regulate apoptosis, inflammation, and vasoconstriction. For example, optineurin interacts with adenoviral E3-14.7K protein which protects cells from the cytolytic activity of TNF-α.[21] Huntingtin is linked to the Rab8 protein through optineurin, which may regulate membrane traffic and cellular morphogenesis.[25] Vittitow and Borrás[42] studied the effect of glaucomatous insults on the expression of optineurin in a human anterior segment organ culture perfusion system under conditions mimicking physiologic pressure. Sustained elevated IOP, TNF-α exposure, and prolonged dexamethasone treatment significantly upregulated optineurin expression in the trabecular meshwork.

In glaucomatous eyes, the expression of TNF-α and TNF-α receptor-1 was upregulated in the retina and optic nerve head.[43,44] Yuan and Neufeld[45] reported that the expression of TNF-α and TNF-α receptor-1 appeared to parallel the progression of optic nerve degeneration. An association of TNF-α −308G→A polymorphism with POAG has been reported in the Chinese.[46] In this study, we examined three single-nucleotide polymorphisms, −308G→A, −857C→T, and −863C→A, in the TNF-α promoter region in a Japanese population. Transcriptional activity of the −857T allele or −863A allele was significantly greater than that of the −857C allele or −863C allele.[37] However, no significant difference in genotype or allele frequency was noted between patients and control subjects for the three single-nucleotide polymorphisms of the TNF-α gene. Especially, the −308G→A polymorphism is rare in the Japanese.[47]

The genotype frequency of the c.412G→A (Thr34Thr) polymorphism in the *OPTN* gene was significantly associated with POAG, and the frequency of 412A carriers was significantly greater in patients with POAG than in control subjects ($P = 0.009$). This association was influenced by TNF-α/−857C→T genotypes (Table 6). Among individuals with the C/T+T/T genotype (or −857T carriers) in the TNF-α gene, the frequency of optineurin/412A carriers was significantly greater in patients with POAG than in control subjects (odds ratio 2.86, $P = 0.006$). The visual field scores at diagnosis in patients with POAG were significantly worse in patients with optineurin/412A when they were TNF-α/−857T carriers ($P = 0.020$; Table 7), although we found no significant difference in the scores between the c.412G→A genotypes in the *OPTN* gene ($P = 0.093$, Table 4).

The same interactions were more clearly observed between the c.603T→A (Met98Lys) polymorphism in the *OPTN* gene and the −863C→A polymorphism in the TNF-α gene. Although there was no significant association between c.603T→A (Met98Lys) polymorphism and POAG or NTG, the frequency of optineurin/603A carriers was significantly greater in patients with POAG (odds ratio, 4.11; $P = 0.008$) than in control subjects and in patients with NTG (odds ratio, 3.31; $P = 0.027$) than in control subjects among individuals with the C/A+A/A genotype (or −863A carriers) in the TNF-α gene. The visual field scores at diagnosis in patients with POAG were significantly worse in patients with optineurin/603A (or Lys98) when they were TNF-α/−863A carriers ($P = 0.026$). However, there was no significant difference in visual field score at

TABLE 7. Comparison of Clinical Characteristics of Glaucoma Patients According to TNF-α Genotypes (−857T and −863A) and Optineurin Genotypes (c.412G→A and c.603T→A)

	(TNF-α Genotypes) (*OPTN* Genotypes)	C/T + T/T (−857T Carrier) G/G	C/T + T/T (−857T Carrier) G/A + A/A	*P**
c.412G→A (Thr34Thr)				
POAG	Age at diagnosis (y)	57.1 ± 10.7 (n = 32)	57.6 ± 13.1 (n = 26)	0.802
	IOP at diagnosis (mm Hg)	26.4 ± 6.1 (n = 30)	26.4 ± 5.5 (n = 20)	0.786
	Visual field score	2.9 ± 0.9 (n = 33)	3.3 ± 0.8 (n = 26)	0.020*
NTG	Age at diagnosis (y)	58.4 ± 11.1 (n = 51)	59.3 ± 10.5 (n = 18)	0.790
	IOP at diagnosis (mm Hg)	16.4 ± 2.6 (n = 46)	16.1 ± 2.3 (n = 17)	0.520
	Visual field score	2.8 ± 0.8 (n = 51)	2.6 ± 0.5 (n = 18)	0.335
	(TNF-α Genotypes) (*OPTN* Genotypes)	C/A + A/A (−863A Carrier) T/T	C/A + A/A (−863A Carrier) T/A + A/A	*P**
c.603T→A (Met98Lys)				
POAG	Age at diagnosis (y)	56.3 ± 10.5 (n = 38)	62.0 ± 13.8 (n = 15)	0.074
	IOP at diagnosis (mm Hg)	27.9 ± 6.5 (n = 36)	26.9 ± 8.7 (n = 14)	0.488
	Visual field score	3.0 ± 0.8 (n = 38)	3.5 ± 0.9 (n = 15)	0.026*
NTG	Age at diagnosis (y)	57.9 ± 11.4 (n = 44)	56.9 ± 11.9 (n = 14)	0.579
	IOP at diagnosis (mm Hg)	16.2 ± 2.4 (n = 40)	16.9 ± 2.4 (n = 14)	0.364
	Visual field score	2.9 ± 0.5 (n = 44)	2.7 ± 0.6 (n = 14)	0.296

* $P < 0.05$, Mann-Whitney test.

diagnosis in patients with POAG among the four different genotypes of combined TNF-α/−857T→A and optineurin/412G→A polymorphisms, or TNF-α/−863C→A and optineurin/603T→A polymorphisms in Table 6, by one-way ANOVA ($P = 0.152$ or $P = 0.200$, respectively). These results suggest an association between the visual field scores at diagnosis and combination of the TNF-α/−857C→T and optineurin/412G→A genotypes, or TNF-α/−863C→A and optineurin/603T→A genotypes.

In conclusion, the His26Asp mutation in the *OPTN* gene is a possible disease-causing mutation in Japanese patients with open-angle glaucoma. The c.412G→A polymorphism was significantly associated with POAG and NTG, and the c.603T→A (Met98Lys) polymorphism tended to be associated with NTG. Optineurin expression is directly induced by TNF-α. Genetic statistical analysis showed an interaction between single-nucleotide polymorphisms in the TNF-α gene (−857C→T and −863C→A) and those in the optineurin gene (c.412G→A and c.603 T→A), which increases the risk for the development and probably progression of glaucoma in patients with POAG.

Acknowledgments

The authors thank Makoto Nagano in the Research Department of R&D Center, BML for excellent technical assistance with the Invader assay.

References

1. Quigley HA. Number of people with glaucoma worldwide. *Br J Ophthalmol*. 1996;80:389-393.
2. Kocur I, Resnikoff S. Visual impairment and blindness in Europe and their prevention. *Br J Ophthalmol*. 2002;86:716-722.
3. Heijl A, Leske MC, Bengtsson B, et al. The Early Manifest Glaucoma Trial Group. Reduction of intraocular pressure and glaucoma progression: results from the Early Manifest Glaucoma Trial. *Arch Ophthalmol*. 2002;120:1268-1279.
4. Wilson. Epidemiology of chronic open-angle glaucoma. In: Ritch R, Shields MB, Krupin T, eds. *The Glaucomas*. St. Louis: Mosby; 1996;753-768.
5. Friedman JS, Walter MA. Glaucoma genetics, present and future. *Clin Genet*. 1999;55:71-79.
6. Stone EM, Fingert JH, Alward WLM, et al. Identification of a gene that causes primary open angle glaucoma. *Science*. 1997;275:668-670.
7. Kubota R, Noda S, Wang Y, et al. A novel myosin-like protein (myocilin) expressed in the connecting cilium of the photoreceptor: molecular cloning, tissue expression, and chromosomal mapping. *Genomics*. 1997;41:360-369.
8. Alward WLM, Fingert JH, Coote MA, et al. Clinical features associated with mutations in the chromosome 1 open-angle glaucoma gene (GLC1A). *N Engl J Med*. 1998;338:1022-1027.
9. Fingert JH, Héon E, Liebmann JM, et al. Analysis of myocilin mutations in 1703 glaucoma patients from five different populations. *Hum Mol Genet*. 1999;8:899-905.
10. Shimizu S, Lichter PR, Johnson AT, et al. Age-dependent prevalence of mutations at the GLC1A locus in primary open-angle glaucoma. *Am J Ophthalmol*. 2000;130:165-177.
11. Faucher M, Anctil JL, Rodrigue MA, et al. Founder *TIGR/myocilin* mutations for glaucoma in the Québec population. *Hum Mol Genet*. 2002;11:2077-2090.
12. Fingert JH, Stone EM, Sheffield VC, Alward WLM. Myocilin glaucoma. *Surv Ophthalmology*. 2002;47:547-561.
13. Rezaie T, Child A, Hitchings R, et al. Adult-onset primary open-angle glaucoma caused by mutations in optineurin. *Science*. 2002;295:1077-1079.
14. Sarfarazi M, Child A, Stoilova D, et al. Localization of the fourth locus (GLC1E) for adult-onset primary open-angle glaucoma to the 10p15-p14 region. *Am J Hum Genet*. 1998;62:641-652.
15. Forsman E, Lemmelä S, Varilo T, et al. The role of TIGR and OPTN in Finnish glaucoma families: a clinical and molecular genetic study. *Mol Vis*. 2003;9:217-222.
16. Tang S, Toda Y, Kashiwagi K, et al. The association between Japanese primary open-angle glaucoma and normal tension glaucoma patients and the optineurin gene. *Hum Genet*. 2003;113:276-279.
17. Wiggs JL, Auguste J, Allingham RR, et al. Lack of association of mutations in optineurin with disease in patients with adult-onset primary open-angle glaucoma. *Arch Ophthalmol*. 2003;121:1181-1183.
18. Leung YF, Fan BJ, Lam DSC, et al. Different optineurin mutation pattern in primary open-angle glaucoma. *Invest Ophthalmol Vis Sci*. 2003;44:3880-3884.

19. Aung T, Ebenezer ND, Brice G, et al. Prevalence of optineurin sequence variants in adult primary open angle glaucoma: implications for diagnostic testing. *J Med Genet*. 2003;40:e101. Available at http://www.jmedgenet.com/cgi/content/full/40/8/e101.
20. Alward WLM, Kwon YH, Kawase K, et al. Evaluation of optineurin sequence variations in 1,048 patients with open-angle glaucoma. *Am J Ophthalmol*. 2003;136:904-910.
21. Li Y, Kang J, Horwitz MS. Interaction of an adenovirus E3 14.7-kilodalton protein with a novel tumor necrosis factor alpha-inducible cellular protein containing leucine zipper domains. *Mol Cell Biol*. 1998;18:1601-1610.
22. Faber PW, Barnes GT, Srinidhi J, et al. Huntingtin interacts with a family of WW domain proteins. *Hum Mol Genet*. 1998;7:1463-1474.
23. Schwamborn K, Weil R, Courtois G, et al. Phorbol esters and cytokines regulate the expression of the NEMO-related protein, a molecule involved in a NF-κB-independent pathway. *J Biol Chem*. 2000;275:22780-22789.
24. Moreland RJ, Dresser ME, Rodgers JS, et al. Identification of a transcription factor IIIA-interacting protein. *Nucleic Acids Res*. 2000;28:1986-1993.
25. Hattula K, Peränen J. FIP-2, a coiled-coil protein, links Huntingtin to Rab8 and modulates cellular morphogenesis. *Curr Biol*. 2000; 10:1603-1606.
26. Ellis LA, Taylor CF, Taylor GR. A comparison of fluorescent SSCP and denaturing HPLC for high throughput mutation scanning. *Hum Mutat*. 2000;15:556-564.
27. Bunn CF, Lintott CJ, Scott RS, George PM. Comparison of SSCP and DHPLC for the detection of LDLR mutations in a New Zealand cohort. *Hum Mutat*. 2002;19:311. Available at http://www.interscience.wiley.com/humanmutation/pdf/mutation/492.pdf.
28. Brezin AP, Bechetoille A, Hamard P, et al. Genetic heterogeneity of primary open angle glaucoma and ocular hypertension: linkage to GLC1A associated with an increased risk of severe glaucomatous optic neuropathy. *J Med Genet*. 1997;34:546-552.
29. Copin B, Brezin AP, Valtot F, et al. Apolipoprotein E-promoter single-nucleotide polymorphisms affect the phenotype of primary open-angle glaucoma and demonstrate interaction with the myocilin gene. *Am J Hum Genet*. 2002;70:1575-1581.
30. Hosoda M, Hirano T, Tsukahara S. Mode of progression of visual field defects and risk factors in glaucoma patients (in Japanese). *J Jpn Ophthalmol Soc*. 1997;101:593-597.
31. Kozaki J, Kozaki H, Kozaki R. Twenty-year follow-up of visual field defects in primary glaucoma eyes (in Japanese). *J Jpn Ophthalmol Soc*. 1999;103:18-25.
32. Anderson DR, Patella VM. *Automated Static Perimetry*. 2nd ed. St. Louis: Mosby; 1999:164.
33. Narayanaswami G, Taylor PD. Improved efficiency of mutation detection by denaturing high-performance liquid chromatography using modified primers and hybridization procedure. *Genet Test*. 2001;5:9-16.
34. Lyamichev V, Mast AL, Hall JG, et al. Polymorphism identification and quantitative detection of genomic DNA by invasive cleavage of oligonucleotide probes. *Nat Biotechnol*. 1999;17:292-296.
35. Wilson AG, di Giovine FS, Blakemore AI, Duff GW. Single base polymorphism in the human tumour necrosis factor alpha (TNF alpha) gene detectable by NcoI restriction of PCR product. *Hum Mol Genet*. 1992;1:353.
36. Kato T, Honda M, Kuwata S, et al. Novel polymorphism in the promoter region of the tumor necrosis factor alpha gene: no association with narcolepsy. *Am J Med Genet*. 1999;88:301-304.
37. Higuchi T, Seki N, Kamizono S, et al. Polymorphism of the 5'-flanking region of the human tumor necrosis factor (TNF)-[alpha] gene in Japanese. *Tissue Antigens*. 1998;51:605-612.
38. Fuse N, Takahashi K, Akiyama H, et al. Molecular genetic analysis of optineurin gene for primary open-angle and normal tension glaucoma in Japanese population. *J Glaucoma*. 2004;13:299-303.
39. Melki R, Belmouden A, Akhayat O, et al. The M98K variant of the OPTINEURIN (OPTN) gene modifies initial intraocular pressure in patients with primary open angle glaucoma. *J Med Genet*. 2003; 40:842-844.
40. Fairbrother WG, Yeh RF, Sharp PA, Burge CB. Predictive identification of exonic splicing enhancers in human genes. *Science*. 2002;297:1007-1013.
41. Nemesure B, Jiao X, He Q, et al. A genome-wide scan for primary open-angle glaucoma (POAG): the Barbados Family Study of Open-Angle Glaucoma. *Hum Genet*. 2003;112:600-609.
42. Vittitow JL, Borrás T. Expression of optineurin, a glaucoma-linked gene, is influenced by elevated intraocular pressure. *Biochem Biophys Res Commun*. 2002;298:67-74.
43. Yan X, Tezel G, Wax MB, Edward DP. Matrix metalloproteinases and tumor necrosis factor-α in glaucomatous optic nerve head. *Arch Ophthalmol*. 2000;118:666-673.
44. Tezel G, Li LY, Patil RV, Wax MB. TNF-α and TNF-α receptor-1 in the retina of normal and glaucomatous eyes. *Invest Ophthalmol Vis Sci*. 2001;42:1787-1794.
45. Yuan L, Neufeld AH. Tumor necrosis factor-α: a potentially neurodestructive cytokine produced by glia in the human glaucomatous optic nerve head. *Glia*. 2000;32:42-50.
46. Lin HJ, Tsai FJ, Chen WC, et al. Association of tumour necrosis factor alpha −308 gene polymorphism with primary open-angle glaucoma in Chinese. *Eye*. 2003;17:31-34.
47. Allen RD. Polymorphism of the human TNF-α promoter—random variation or functional diversity? *Mol Immunol*. 1999;36:1017-1027.

Early-Onset Macular Degeneration with Drusen in a Cynomolgus Monkey (*Macaca fascicularis*) Pedigree: Exclusion of 13 Candidate Genes and Loci

Shinsuke Umeda,[1,2] *Radha Ayyagari,*[3] *Rando Allikmets,*[4] *Michihiro T. Suzuki,*[5] *Athancios J. Karoukis,*[3] *Rajesh Ambasudhan,*[3] *Jana Zernant,*[4] *Haru Okamoto,*[1] *Fumiko Ono,*[5] *Keiji Terao,*[6] *Atsushi Mizota,*[7] *Yasuhiro Yoshikawa,*[2] *Yasuhiko Tanaka,*[1] *and Takeshi Iwata*[1]

Purpose. To describe hereditary macular degeneration observed in the cynomolgus monkey (*Macaca fascicularis*), which shares phenotypic features with age-related macular degeneration in humans, and to test the involvement of candidate gene loci by mutation screening and linkage analysis.

Methods. Ophthalmic examinations with fundus photography, fluorescein angiography (FA), indocyanine green angiography (IA), electroretinography (ERG), and histologic studies were performed on both affected and unaffected monkeys in the pedigree. The monkey orthologues of the human *ABCA4*, *VMD2*, *EFEMP1*, *TIMP3*, and *ELOVL4* genes were cloned and screened for mutations by single-strand conformation polymorphism (SSCP) analysis or denaturing high-performance liquid chromatography (DHPLC) and direct sequencing in six affected and five unaffected monkeys from the pedigree and in six unrelated, unaffected monkeys. Subsequently, 13 human macular degeneration loci including these five genes were analyzed to test for linkage with the disease. Nineteen affected and seven unaffected monkeys in the pedigree were analyzed by using human microsatellite markers linked to the 13 loci.

Results. Yellowish white spots were observed in the macula and fovea centralis, and in some cases the spots scattered to the peripheral retina along the blood vessels. FA showed hyperfluorescence corresponding to the dots except in the foveola. No anomalies were found by IA and ERG. Histologic studies demonstrated that the spots were drusen. Mutation analysis of the *ABCA4*, *VMD2*, *EFEMP1*, *TIMP3*, and *ELOVL4* genes identified a few sequence variants, but none of them segregated with the disease. Linkage analysis with markers linked to these five genes and an additional eight human macular degeneration loci failed to establish linkage. Haplotype analysis excluded the involvement of the 13 candidate loci for harboring the gene associated with macular degeneration in the monkeys.

Conclusions. Significant homology was identified between monkey and human orthologues of the five macular degeneration genes. Thirteen loci associated with macular degeneration in humans or harboring macular degeneration genes were excluded as causal of early-onset macular degeneration in the monkeys. It is likely that none of these loci, but rather a novel gene, is involved in causing the observed phenotype in this monkey pedigree. (*Invest Ophthalmol Vis Sci.* 2005;46: 683–691) DOI:10.1167/iovs.04-1031

From the [1]National Institute of Sensory Organs, National Hospital Organization Tokyo Medical Center, Tokyo, Japan; the [2]Department of Biomedical Science, Graduate School of Agricultural and Life Sciences, The University of Tokyo, Tokyo, Japan; the [3]Department of Ophthalmology, Kellogg Eye Center, University of Michigan, Ann Arbor, Michigan; the [4]Departments of Ophthalmology and Pathology, Columbia University, New York, New York; The [5]Corporation for Production and Research of Laboratory Primates, Ibaraki, Japan; the [6]Tsukuba Primate Center for Medical Science, National Institute of Infectious Diseases, Ibaraki, Japan; and the [7]Department of Ophthalmology, Juntendo University Urayasu Hospital, Chiba, Japan.

Supported by research grant, Research on Measures for Intractable Diseases, Ministry of Health, Labor and Welfare of Japan and by the fellowship of the Promotion of Science for Japanese Junior Scientists (SU); The Foundation Fighting Blindness (RAl, RAy), National Eye Institute Grants EY13435 (RAl) and EY13198 (RAy), Research to Prevent Blindness (RAl, RAy) and Core Grant EY07003.

Submitted for publication August 27, 2004; revised November 1, 2004; accepted November 5, 2004.

Disclosure: **S. Umeda**, None; **R. Ayyagari**, None; **R. Allikmets**, None; **M.T. Suzuki**, None; **A.J. Karoukis**, None; **R. Ambasudhan**, None; **J. Zernant**, None; **H. Okamoto**, None; **F. Ono**, None; **K. Terao**, None; **A. Mizota**, None; **Y. Yoshikawa**, None; **Y. Tanaka**, None; **T. Iwata**, None

The publication costs of this article were defrayed in part by page charge payment. This article must therefore be marked "*advertisement*" in accordance with 18 U.S.C. §1734 solely to indicate this fact.

Corresponding author: Takeshi Iwata, National Institute of Sensory Organs, National Hospital Organization Tokyo Medical Center, 2-5-1 Higashigaoka, Meguro-ku, Tokyo 152-8902 Japan; iwatatakeshi@kankakuki.go.jp.

Copyright © Association for Research in Vision and Ophthalmology

The inherited macular dystrophies comprise a heterogeneous group of blinding disorders characterized by central visual loss and atrophy of the macula and underlying retinal pigment epithelium (RPE).[1] The complexity of the molecular basis of monogenic macular disease is being elucidated through identification of many of the disease-causing genes.[2–8] Because of limitations associated with studies in humans, nonhuman species with phenotypes similar to human macular degeneration have been used as model systems to study these diseases. Rodent models generated by altering the genes homologous to the disease-causing genes in humans are most extensively used in such studies; however, rodents do not have a defined macula and, hence, the clinical symptoms observed in humans with macular degeneration cannot be fully replicated.[9–11] Because the macula is found only in primates and birds, a monkey model of macular degeneration would be extremely valuable for studies elucidating the mechanism and etiology underlying these diseases. A primate model for macular degeneration is much needed to develop sensitive diagnostic techniques and potential therapeutic strategies to cure or prevent the disease. Furthermore, such models are of particular value if their genetic basis is understood.

Macular degeneration in monkeys was first described by Stafford in 1974.[12] He reported that 31 (6.6%) of eyes of elderly monkeys showed pigmentary disorders and/or drusen-like spots. In 1978, El-Mofty et al.[13] reported a high incidence (50%) of maculopathy in a closed rhesus monkey colony at the

Caribbean Primate Research Center of the University of Puerto Rico. The latest report from the center states that specific maternal lineages have a statistically significant higher prevalence of drusen.[14] Although they suspected the involvement of hereditary factors, genetic analysis of the macaque population has not been reported.

We have reported a high incidence of macular degeneration in one of the cynomolgus monkey (*Macaca fascicularis*) colonies at the Tsukuba Primate Center.[15,16] This macular degeneration originated from one affected male monkey, which showed phenotypic characterization of macular degeneration. The disease affects the central retina specifically, with yellowish white dots in the macula and lipofuscin deposits in the RPE, consistent with the phenotype observed in the early stages of age-related macular degeneration (AMD). These symptoms appear at the age of ~2 years and progress slowly throughout life. Mating experiments have demonstrated that this familial macular degeneration is segregating as an autosomal dominant trait.[17]

AMD is currently considered a multifactorial disorder involving both environmental and genetic factors. Recent studies have substantiated the evidence for AMD as a complex genetic disorder in which one or more genes contribute to an individual's susceptibility to the development of the disease.[18–20] To date, full-genome scan studies have indicated that some regions of the genome harbor AMD-predisposing genes.[21,22] However, most genes associated with susceptibility to AMD have not been identified, presumably because of a complex pattern of inheritance, late age of onset, and difficulties in obtaining large pedigrees for standard linkage analysis. Genes implicated in monogenic macular dystrophies that occur earlier in life with a clear pattern of inheritance have been considered as good candidates for susceptibility to AMD.[23–26] To date, 15 macular degeneration genes have been linked or cloned for human macular degeneration (RetNet; http://www.sph.uth.tmc.edu/Retnet/home.htm; provided in the public domain by University of Texas Houston Health Science Center, Houston, TX). However, with the exception of *ABCA4*, none of these genes has shown a convincing association with AMD.

Because the monkey macular degeneration model we present here shares phenotypic similarities with the early stages of AMD, the identification of the gene involved in this monkey pedigree may provide critical clues to the understanding of the mechanism of AMD. In this study, monkey orthologues of the human genes responsible for Stargardt macular degeneration 1 (*ABCA4*),[2] Best macular degeneration (*VMD2*),[3,7] Doyn honeycomb dystrophy (*EFEMP1*),[4] Sorsby fundus dystrophy (*TIMP3*),[5] and Stargardt macular degeneration 3 (*ELOVL4*)[6,8] were cloned and screened for mutations in the affected monkeys. Subsequently, 13 human macular degeneration loci, including these five genes, were analyzed to test for linkage with the disease in the pedigree. During this process, we evaluated the nature and utility of human microsatellite markers in the cynomolgus monkey for linkage studies. This article also describes the gene structure and evolutionary conservation of the five human macular degeneration genes in the cynomolgus monkey.

Materials and Methods

Maintenance of Monkeys

The cynomolgus monkeys in the pedigree with macular degeneration were reared at the Tsukuba Primate Center for Medical Science (National Institute of Infectious Diseases; Tokyo, Japan). All monkeys were treated in accordance with the rules for care and management of animals at the Tsukuba Primate Center[27] under the Guiding Principles for Animal Experiments using Non-Human Primates formulated and enforced by the Primate Society of Japan (1986). All experimental procedures were approved by the Animal Welfare and Animal Care Committee of the National Institute of Infectious Diseases of Japan. These animal protocols fulfill the guidelines in the ARVO Statement for the Use of Animals in Ophthalmic and Vision Research.

Clinical Studies

Fundus photographs, fluorescein angiography (FA), and indocyanine green angiography (IA) were performed with a fundus camera (TRC50; Topcon, Tokyo, Japan) in animals under anesthesia. Electroretinography (ERG) was recorded in four affected and six normal monkeys with a white/color LED stimulator and contact lens electrode (LS-W; Mayo, Aichi, Japan). After 20 minutes of dark adaptation, rod ERG, combined ERG, and oscillatory responses were recorded, and single-flash cone response and 30-Hz flicker ERG were recorded after 10 minutes of light adaptation. The stimulus and recording conditions conformed to the standards for clinical electroretinography recommended by the International Society for Clinical Electrophysiology of Vision.[28]

Genomic DNA and RNA Isolation

Peripheral blood was collected from 19 affected and 11 unaffected monkeys from the pedigree (Fig. 1, asterisks, pound signs) and an

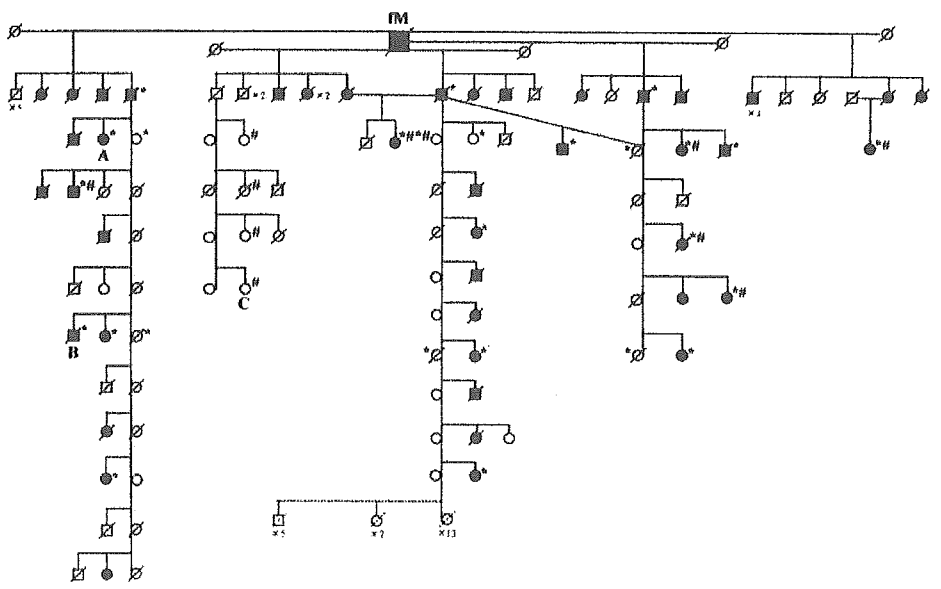

FIGURE 1. Edited version of the monkey pedigree with macular degeneration: fM, the founder breeding male monkey with typical macular degeneration, is shown with five healthy mates arrayed horizontally. The first-generation offspring are also arrayed horizontally. The breeding members from each branch of the first generation offspring are arrayed vertically with their mates and progeny. Monkeys used for *linkage analysis and #mutation screening are marked.

TABLE 1. Primer Sets Used for Cloning of the Monkey Homologues

Gene	Amplified Region	Name	Forward Primer	Position	Name	Reverse Primer	Position	Size (kb)
VMD2	Exon 1	P1F	GACCAGAAACCAGGACTGTTGA	Intron	P1R	GAACTCGCCATATAGCAGCTT	Exon 2	2.1
	Exon 2	P2F	GCTCTGACCAGGGTCTCTGA	Intron	P3R	CCGCACCTTTCCCTGAACTA	Intron	4.5
	Exon 3	P3F	CTAGACCTGGGGACAGTCTCA	Intron	P3R	CCGCACCTTTCCCTGAACTA	Intron	0.3
	Exon 4-5	P4F	CACGGAAGAACAACAGCTGA	Exon 3	P5R	ACACCAGTGGGATACTAATCCAG	Exon 6	2.3
	Exon 6	P6F	GCCAGGAATGGACCATGAGTA	Intron	P6R	GAGCCACTTAGCCTCTAGGTGA	Intron	0.3
	Exon 7-8	P7F	CCTGGAGCATCCTGATTTCA	Intron	P8R	TGAGGCCTCCCTACAGAACA	Intron	2.3
	Exon 9	P9F	TGGCAGAGCAGCTCATCA	Exon 8	P9R	AGCTTCCAGGCCTTGTTG	Exon 10	3.0
	Exon 10	P10F	AAGGGAGAAGGCCAGGTGTT	Intron	P10R	TTTCCTGTAGTGCTTGGGTACTA	Intron	1.2
	Exon 11	P11F	TGCCCTCCTACTGCAACATT	Intron	P11R	ATGCAATGGAGTGTGCATTA	Intron	1.1
EFEMP1	Exon 1	P1F	TTCTAGAACCCTCTGGTCTCTGA	Intron	P1R	CGCTTTCTTAACAGCAAGCTAAC	Intron	0.9
	Exon 2	P2F	GATTGGAAGTTGAGTATGGTGGA	Intron	P2R	CATTCTAGGGATAATGTGGTACCAA	Intron	1.3
	Exon 3-4	P3F	AAGATGGTACTGGGCAACTGTAC	Intron	P4R	ACATCTGTAGAGTAGCTTGACAGCA	Intron	1.4
	Exon 5	P5F	CTACACAGGCTAGAGGAATATGATCA	Intron	P5R	GACACAGGATTTAAGTAACTTGCTCA	Intron	1.3
	Exon 6-7	P6F	CACTGAATGGCATGAACATTG	Intron	P7R	TAGAACAGAATTCCCATGGGTAA	Intron	1.6
	Exon 8	P8F	AATAGGACAAGAAGCCAGATCTCT	Intron	P8R	TTCCTGGTTAAAACTAAATACCTAACA	Intron	0.4
	Exon 9-10	P9F	AACAGATGAACAATAGGTGCTTGA	Intron	P10R	TATCTATCTGGCAGTGTTACCAAGA	Intron	0.9
	Exon 11	P11F	GTATTAGACAAGGGATAAGAGCCAA	Intron	P11R	CAGAGGTTATGCATATATGCTGTGA	Intron	1.7
TIMP3	Exon 1	P1F	CCCAGGGCTATATCACTCG	Intron	P1R	AGCCACTGTGAGTTTCCTCTG	Intron	0.7
	Exon 2	P2F	CAATGGCTCTAACAGGAGAAGTAG	Intron	P2R	CTTGACGAAGGTCTCATGGTTA	Intron	0.8
	Exon 3-4	P3F	TCCAGTTCCAGCTGCATTG	Intron	P4R	AGTTAGTGTCCAAGGGAAGCT	Exon 5	2.6
	Exon 5	P5F	ATGTAGCGAGGCTTGACCAA	Exon 3	P5R	AGGTGAGCTAAACACTATTCTGGA	Intron	3.5

additional six unrelated normal monkeys, and genomic DNA was extracted (QIAamp DNA Blood Maxi Kit; Qiagen, Valencia, CA). A normal monkey outside the pedigree was killed for bilateral eye enucleation, and enucleated eyes were immersed and stored in RNA-stabilization solution (RNAlater; Ambion, Austin, TX) at −80°C until RNA isolation. After thawing on ice, the eyeballs were dissected to separate the neural retina and choroid followed by extraction of total RNA.

Histologic Studies

An affected 14-year-old male monkey (Fig. 1, monkey B) was killed for histologic studies. Enucleated eyes were fixed in 10% neutralized formaldehyde solution at 4°C overnight, dehydrated, and embedded in paraffin. Four-micrometer-thick sections were prepared and stained with hematoxylin and eosin (HE) or periodic acid–Schiff (PAS). Serial sections were used for immunohistochemical analysis with anti-complement 5 (C5) antibody. After pretreatment with 0.4 mg/mL proteinase K in phosphate-buffered saline (PBS) for 5 minutes and blocking with 5% skim milk in PBS for 20 minutes at room temperature, the sections were incubated with rabbit anti-human C5 polyclonal antibody (Dako, Glostrup, Denmark) diluted to 1:200 dilution in PBS for 2 hours at room temperature. Alexa 488–conjugated goat anti-rabbit IgG (Molecular Probes, Eugene, OR), diluted to 1:200 in PBS, was used as the secondary antibody. The negative control experiments were performed using normal rabbit immunoglobulin fraction (Dako) instead of anti-C5 antibody.

Characterization of the Genomic Organization and cDNA Sequence of the Monkey *ABCA4*, *VMD2*, *EFEMP1*, and *TIMP3* Genes

Gene-specific primers of the human macular degeneration genes *ABCA4*, *VMD2*, *EFEMP1*, and *TIMP3* were designed based on the human genomic DNA sequence to amplify exons of monkey genes (Table 1). Amplified products were directly sequenced. For all genes except *ABCA4*, the 5′/3′-rapid amplification of cDNA ends (5′/3′-RACE) was performed using total RNA isolated from the monkey retina. Amplification of partial cDNAs by both 5′- and 3′-RACE was designed to generate overlapping PCR products to obtain a full-length cDNA sequence. Primers were initially designed based on the exonic sequences obtained by genomic sequence (Table 2). RACE products were subcloned into the pCRII cloning vector (TA Cloning Kit Dual Promoter; Invitrogen, Carlsbad, CA) and sequenced directly. The obtained nucleotide sequence data have been submitted to GenBank, and assigned accession numbers: *TIMP3*: AY207381–207385, AH012631; *EFEMP1*: AY312407–312415, AH012997; *VMD2*: AY357925–357936, AH013172; *ELOVL4*: AF461182–461187, AH012403; *ABCA4*; AY793687 (http://www.ncbi.nlm.nih.gov/Genbank; provided in the public domain by the National Center for Biotechnology Information, Bethesda, MD).

Mutation Analysis

Coding regions and adjacent intronic sequences of the monkey *ABCA4*, *VMD2*, *EFEMP1*, *TIMP3*, and *ELOVL4* genes were analyzed for sequence variants by single-strand conformation polymorphism (SSCP) or denaturing (D)HPLC (for the *ABCA4* gene) analysis in parallel with direct sequencing. Genomic DNA from six affected and five unaffected monkeys from the pedigree (Fig. 1, pound signs) and six unrelated normal subjects were used for mutation analysis. Primers located in the intronic regions were designed to amplify coding sequences of individual genes (Table 3). Large exons were divided into smaller segments to obtain amplification products suitable for SSCP analysis. The purified amplicons were analyzed by SSCP or DHPLC analysis, as previously described.[29,30] All the samples were also analyzed by bidirectional sequencing with the PCR primers. Exons 2, 7, and 10 of the *VMD2* gene were screened for sequence variants only by direct sequencing.

TABLE 2. Primers for 5′-3′-RACE

Gene	5′-RACE	Position	3′-RACE	Position
VMD2	GTATACACCAGTGGGATA	Exon 6	AGAGCAACAGCTGATGTTTGAGAA	Exon 3
EFEMP1	GGATGGTACATTCATCTA	Exon 7	GATCCTGTGAGACAGCAATGCA	Exon 3
TIMP3	ATCATCTGGGAAGAGTTA	Exon 5	GATGAAGATGTACCGAGGCTTCA	Exon 2–3

TABLE 3. Primer Sets Used for Mutation Screening

Gene	Exon No.	Length (bp)	Name	Forward Primer	Name	Reverse Primer	Size (bp)
ABCA4	1	66	01F	TCTTCGTGTGGTCATTAGC	01R	ACCCCACACTTCCAACCTG	152
	2	94	02F	AAGTCCTACTGCACACATGG	02R	CTAGACAAAAGGCCCAGACC	266
	3	142	03F	TTCCCAAAAAGGCCAACTC	03R	CACGCACGTGTGCATTTCAG	301
	4	139	04F	GCTATTTCCTTATTAATGAGGC	04R	GGGAAATGATGCTTGAGAGC	212
	5	128	05F	CCCTTCAACACCCTGTTCTT	05R	TTCTTGCCTTTCTCAGGCTGG	237
	6	198	06F	GTATTCCCAGGTTCTGTGG	06R	TACCCCAGGAATCACCTTG	330
	7	88	07F	AGCATATAGGAGATCAGACTG	07R	GGCATAAGAGGGGTAAATGG	241
	8	238	08F	GAGCATTGGCCTCACAGCAG	08R	CCCCAGGTTTGGTTTCACC	397
	9	139	09F	AGACATGTGATGTGGATACAC	09R	GTGGGAGGTCCAGGGTACAC	271
	10	117	10F	AACACTAAGTGATAGGGGCAGAA	10R	GGCCTGCTTGTTGTATTTTGAT	344
	11	198	11F	AGCTCACTCGCTCTTTAGGG	11R	TTCAAGACCACTTGACTTGC	406
	12	206	12F	TGGGACAGCAGCCCTTATC	12R	CCAAATGTAATTTCCCACTGAC	362
	13	177	13F	AATGAGTTCCGAGTCACCCTG	13R	CCCATTAGCGTGTCATGG	308
	14	223	14F	TCCATCTGGGCTTTGTTCTC	14R	AATCCAGGCACATGAACAGG	407
	15	222	15F	AGACAGTAACTAACAGGCTCGTG	15R	GGACTGCTACAGACCCTTCC	386
	16	205	16F	CTGTTGCATTGGATAAAAGGC	16R	GATGAATGGAGAGGGCTGG	330
	17	65	17F	CTGCGGTAAGGTAGGATAGGG	17R	CACACCGTTTACATAGAGGGC	232
	18	90	18F	CAGCTCCCGGTGGTAGAGTA	18R	CGCTTGCCATGAGATGTTTT	222
	19	175	19F	TGGGGCCATGTAATTAGGC	19R	TGGGAAAGAGTAGACAGCCG	322
	20	132	20F	GCATGTTGCTAAAGGCCATC	20R	TATCTCTGCCTGTGCCCAG	293
	21	140	21F	GTAAGATCAGCTGCTGGAAG	21R	GAAGCTCTCCTGCTCCAAGC	301
	22	138	22F	CCCTCCACAGTCCCTTAACTC	22R	GAGAGTGGGGACCACAGGTA	244
	23	194	23F	TTTTGCAACTATGTAGCCAGGA	23R	AGCCTGTGTGAGTAGCCATG	384
	24	85	24F	GCATCAGGGAGAGGCTGTC	24R	CCCAGCAATATTGGGAGATG	212
	25	206	IVS24F	GTAAGGACTGGACGGGCCATACTTGG	IVS24R	TCCAGCTCTCTGAAAAGGCTGGCATA	2 kb
			IVS25F	AAAGCTGGTGGAGTGCATTGGTCAAG	IVS25R	CCTGAATCAGAATCCTCCGTGACCTTC	500
	26	49	26F	TCCCATTATGAAGCAATAGC	26R	ACCCAGCCCCTTAGACTTTC	228
	27	266	IVS26F	GGATTCTGATTCAGGACCTCTGTTTGC	IVS26R	CTGCGGATGGTGTGTTGGAATCTCTT	2 kb
			IVS27F	TCCCAGAGAGAAGGCTGGACAGACAC	IVS27R	CCCATATATCCAGGGGTGAAGGGTCA	1 kb
	28	125	28F	TGCACGCGCACGGTGTGAC	28R	TGAAGGTCCCAGTGAAGTGGG	291
	29	99	29F	CAGCAGCTATCCAGTAAAGG	29R	AACGCCTGCCATCTTGAAC	263
	30	187	30F	GTTGGGCACAATTTCTTATGC	30R	ACTCAGGAGATACCAGGGAC	347
	31	95	IVS30F	GAGAAGCTCACCATGCTGCCAGAGT	IVS30R	GAGATGTTCCTGTCCGTCAGGTCTTG	2 kb
			IVS31F	CGCAGCACGGAAATTCTACAAGACCT	IVS31R	CCTCTGTTCATTGACCCAGAATTTGCT	700
	32	33	32F	ACGGCACTGCTGTACTTGTG	32R	TCAACATGGCTGTGAGGTGT	182
	33	106	IVS32F	GAGCAAATTCTGGGTCAATGAACAGAGG	IVS32R	CGCTTAAAAACCCAACAAGTGCTTCC	1.2 kb
			IVS33F	AGGTATGGAGGAATTTCCATTGGAGGA	IVS33R	CTTTAGAGGCCTCTCTAGTGATAGG	300
	34	75	34F	AAACCGTCTTGTTTGTTTGTTT	34R	AGGAGGGAGGGAATTCAATG	208
	35	170	IVS34F	GGCCCTATCACTAGAGAGGCCTCTAAAG	IVS34R	GGTTGGCTAATGACGGTGATTCCATAC	550
			IVS35F	CATGCCCTGGTCAGCTTTCTCAATGT	IVS35R	GAGAAAATCACGCAGATGGCAACCAC	2 kb
	36	178	36F	TGTAAGGCCTTCCCAAAGC	36R	TGGTCCTTCAGAGCACACAC	346
	37	116	37F	CATTTTGCAGAGCTGGCAGC	37R	CTTCTGTCAGGAGATGATCC	260
	38	158	38F	GGAGTGCATTATATCCAGACG	38R	CCTGGCTCTGCTTGACCAAC	302
	39	125	39F	TGCTGTCCTGTGAGAGCATC	39R	CTTCCAGCCCAACAAGGTC	344
	40	130	IVS39F	CTGCTCATTGTCTTCCCCCACTTCTG	IVS39R	CAGCAGGGTCAGGAGGAAGTACACCA	700
			IVS40F	GTGAGGAGCACTCTGCAAATCCGTTC	IVS40R	AGATGAGGAAAAGGGGTCAGGATTGG	3.5 kb
	41	121	41F	GAAGAGAGGTCCCATGGAAAGG	41R	GCTTGCATAAGCATATCAATTG	299
	42	63	42F	CTCCTAAACCATCCTTTGCTC	42R	AGGCAGGCACAAGAGCTG	214
	43	107	43F	GGTCTCTAGGGCCAGGCTA	43R	CACATCTTTCAGGGCCTCAG	271
	44	142	44F	GAAGCTTCTCCAGCCCTAGC	44R	TGCACTCTCATGAAACAGGC	277
	45	135	IVS44F	ACATCTTTACCTTTATGCCCGGCTTCG	IVS44R	AATGAGTGCGATGGCTGTGGAGAGTT	4 kb
			IVS45F	TTAAGAGCCTGGGCCTGACTGTCTACG	IVS45R	GAATCTCTTGCCTGTGGGATGTGAGG	1 kb
	46	104	48F	GAAGCAGTAATCAGAAGGGC	46R	GCCTCACATTCTTCCATGCTG	257
	47	93	47F	TCACATCCCACAGGCAAGAG	47R	TTCCAAGTGTCAATGGAGAAC	258
	48	250	48F	ATTACCTTAGGCCCAACCAC	48R	ACACTGGGTGTTCTGGACC	365
	49	87	49F	GGTGTAGGGTGGTGTTTTCC	49R	ACTGCCTCAAGCTGTGGACT	187
VMD2	2*	152	P2F	GCTCTGACCAGGGTCTCTGA	P3R	CCGCACCTTTCCCTGAACTA	4.5 kb
	3	95	P3F	CTAGACCTGGGGACAGTCTCA	P3R	CCGCACCTTTCCCTGAACTA	325
	4	234	MP4aF	TGGGAGACAGAACCCTTGGA	MP4aF	GTCCTTGCCTTCCACGAA	302
			MP4bF	TGGTGGAACCAGTACGAGAA	MP4bF	TCCACCCATCTTCCATTGTT	286
	5	155	MP5F	AAAGGAGTGCTGAGGTTCCTATA	MP5R	CTTGTTTCCTGTGAACCACAA	330
	6	78	P6F	GCCAGGAATGGACCATGAGTA	P6R	GAGCCACTTAGCCTCTAGGTGA	292
	7*	153	P7F	CCTGGAGCATCCTGATTTCA	P8R	TGAGGCCTCCCTACAGAACA	2.3 kb
	8	81	MP8F	GCATCATGTGGTGTGGAAAT	P8R	TGAGGCCTCCCTACAGAACA	270
	9	152	MP9F	CAAGTCATCAGGCACGTACAA	MP9R	CTAGGCAGACCCCTGCTACTA	286
	10*	639	P10F	AAGGGAGAAGGCCAGGTGTT	P10R	TTTCCTGTAGTGCTTGGGTACTA	1.2 kb
	11	19	P11F	TGCCCTCCTACTGCAACATT	MP11R	AAGTAGTCCTGGACTGCTGATTT	270
EFEMP1	2	81	MP2F	CCGCAGCAGATACTAAATATCAG	MP2R	CCGCTGAACCGTACTTATTTC	173
	3	49	MP3F	CTTAGGGAATGGACACACGAA	MP3R	ACAGAAGGCCAAAGATCACAT	155

(*continues*)

TABLE 3. (*continued*).

Gene	Exon No.	Length (bp)	Name	Forward Primer	Name	Reverse Primer	Size (bp)
	4	387	MP4aF	CCCTCTTAGAAGATTCCTGACTTA	MP4aR	ACACTCCACTGGTTGCCAT	249
			MP4bF	ATGAACAGCCTCAGCAGGA	MP4bR	GCAAAAGCTTTCGATGGTTA	316
	5	123	MP5F	GGAGGCAATATCAACATCTTCA	MP5R	TGCTTGAGGTTGAAACAGTTAAG	248
	6	120	MP6F	GCAAACAGCAATGCTAATTCA	MP6R	GAAATACTGCAACATGGCATG	250
	7	120	MP7F	CAGCTAGGGAATTATTTATCAGCA	MP7R	CAGGGATTGGACTTTATTCCA	279
	8	120	MP8F	ATATCCAAAGTAGTGGTGCACAA	P8R	TTCCTGGTTAAAACTAAATACCTAACA	235
	9	124	MP9F	TGCAAACAGAATCTGCCAGTA	MP9R	TTTGGCTTGGTAAGACCAGAA	265
	10	196	MP10F	CTTACCAAGCCAAACTGCTAACTA	MP10R	AACAAACTCCCATCTTTCTCAATAG	289
	11	162	MP11F	AAAGCATAGAAACTCCAATGCA	MP11R	AGGTAACAATATTCTTTGGCTGACT	281
ELOVL4	1	100	MP1F	CCGCGGTTAGAGGTGTTC	MP1R	GAGACCAGGGGTCGGTGAC	281
	2	188	MP2aF	TTGAGACATCTTGATTCCTAGAAAG	MP2aR	AAGTTAAGCAAAACCATCCCA	252
			MP2bF	CTGGGTCCAAAGTGGATGAA	MP2bR	AGCTAACAGTTATGTCTGGGTACAA	213
	3	81	MP3F	GCAATTGGAATGCATGACA	MP3R	TTTCACAGATTGGGGCCTATA	304
	4	172	MP4aF	AAATGATTCCATGCCTTGTACA	MP4aR	AACGCAAGCAGTATATTCCTGA	330
			MP4b	TGGTGTTTATAACACGCTTTCC	MP4bR	CTCATTGCTTTCCACTGAACA	271
	5	128	MP5F	ATCTCGGTGGCTTACTGCTTA	MP5R	AATAAGTCGGCTGGAGTCAACT	356
	6	276	MP6aF	TTGGGCCTGTGATAGCTATG	MP6aR	TTAGGCTCTTTGTATGTCCGAA	247
			MP6bF	CTCTAATTGCCTACGCAATCAG	MP6bR	GGGAGTTTTTCCTCACTGTCA	242
TIMP3	1	121	MP1F	AACTTTGGAGAGGCGAGCA	MP1R	CCTAAGCAGCGCTGCAGTC	233
	2	83	MP2F	TGAGATGCTGTTCCTGATGTG	MP2R	GGCTGGTGCTTAGACACACA	266
	3	112	MP3F	AGCAGTGGGATTATGGATCATAC	MP3R	ACATTTGGTGAGTCAGCTACTCA	267
	4	122	MP4F	TGGGCTAAGTGGGAACATAGTA	MP4R	GTTTCTAGGGCTGCAAGTCA	274
	5	198	MP5F	TACCATGGCAGATTCCATCA	MP5R	AGTTAGTGTCCGAGGGAAGCT	306

* Exon 2, 7, and 10 of the *VMD2* gene were screened for sequence variants only by direct sequencing.

Linkage Analysis

Linkage analysis was performed on DNA from 19 affected and 7 unaffected members of the pedigree. Individuals used for the analysis are indicated by asterisks in Figure 1. Human microsatellite markers linked to human macular degeneration loci were analyzed with monkey genomic DNA used as the template. Details of microsatellite markers and their primer sequences were obtained from the genome database. Microsatellite marker analysis was performed by two methods: Markers linked to candidate gene loci and included in a linkage mapping set (ver. 2.5MD10; Applied Biosystems, Inc. [ABI], Foster City, CA) were analyzed on the a DNA sequencer (model 3100; ABI) with fluorescence-labeled primers. Additional microsatellite markers were analyzed by ^{32}P dCTP incorporation into the amplified product.[31] Two-point linkage analysis was performed between the disease locus and microsatellite markers with the MLINK program of the LINKAGE package, as described elsewhere.[32,33] Linkage was assessed under the conditions of autosomal dominant inheritance of the disease trait with a frequency of 0.001 for the disease-causing allele, by using the affecteds-only model, as published earlier.[34] Linkage analysis was performed assuming equal frequencies for marker alleles. Haplotypes were constructed with genotypes of microsatellite markers according to their order on human chromosomes.

RESULTS

Clinical and Histologic Findings

Fundus photographs and FA of a 14-year-old female affected monkey (Fig. 1, monkey A) are shown in Figure 2. Fine, yellowish white dots were observed in the maculae (Figs. 2a–d), scattered in the peripheral retina along blood vessels in this monkey (Figs. 2a, 2b). However, in most cases, the locations of the lesions fell within the region centered on the fovea centralis with the same diameter as one optic disc. FA showed hyperfluorescence corresponding to these dots, except foveola (Figs. 2e, 2f). No abnormalities were found in the optic disc, retinal blood vessels, or choroidal vasculatures in any eyes examined. The amplitude and peak latency of both dark- and light-adapted ERG showed no alteration compared with normal control eyes, indicating that global rod or cone degeneration was absent. Histologic studies demonstrated that there were various-sized drusen, weakly stained by PAS (light purple), between the RPE and choriocapillaris in the macular region (Figs. 3a, 3b, asterisk). These drusen were strongly reactive with antibodies against complement C5 (Figs. 3c, 3d). This finding was consistent with the property of drusen reported in patients with AMD.[35] Accumulation of lipofuscin in RPE cells was also obvious by PAS (Figs. 3a, 3b, deep purple, arrows).

Mutation Analysis of the *ABCA4*, *VMD2*, *EFEMP1*, *TIMP3*, and *ELOVL4* Genes

To evaluate the involvement of the *ABCA4*, *VMD2*, *EFEMP1*, *TIMP3*, and *ELOVL4* genes in disease, we first determined the genomic sequence and the complete cDNA sequence of the orthologous genes in the monkey. Subsequently, these genes were screened for sequence variants in affected and unaffected monkeys in the pedigree, in addition to unrelated, unaffected animals by SSCP, or by DHPLC for the *ABCA4* gene, analysis and direct sequencing.

ABCA4. The monkey *ABCA4* gene consists of 50 exons, with its translation stop codon in exon 50, similar to the human gene. The complete 6819-bp cDNA encodes a protein of 2273 amino acids. *ABCA4* is a member of the superfamily of ATP-binding cassette (ABC) transporters, which are associated with membranes and transport various molecules across extra- and intracellular membranes of all cell types. ABC genes typically encode four domains that include two conserved ATP-binding domains and two domains with multiple transmembrane segments. Comparative sequence analysis revealed that the monkey ABCA4 protein was only 1.8% (41 amino acids) different from the human orthologue, whereas the sequence was identical in the two adenosine triphosphate (ATP)-binding domains. Five of the 41 nonconserved amino acids in the monkey protein (codons 223, 423, 1300, 1817, and 2255) involve polymorphisms in the human. Surprisingly, the Lys223Gln and Arg1300Gln changes reported to be associated with Stargardt disease in humans were observed in the homozygous state in

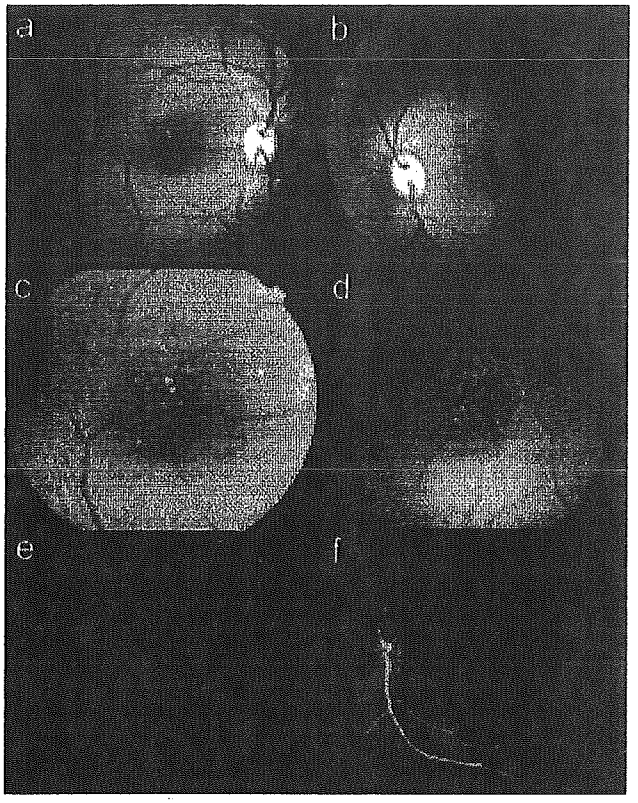

FIGURE 2. Fundus photographs and fluorescein angiogram (FA) of a 14-year-old female cynomolgus monkey (Fig. 1, monkey A) with macular degeneration, showing the right (**a**, **c**, **e**) and left (**b**, **d**, **f**) posterior poles. Fine *grayish white* or *yellowish white* dots were visible in the macula (**a**–**d**). The dots were observed in the peripheral retina along blood vessels in this monkey (**a**, **b**). These dots showed hyperfluorescence in FA except in the foveola (**e**, **f**). High-magnification of the macular region (**c**, **d**, **e**).

one normal control monkey (Fig. 1, monkey C). In addition, the mutation analysis revealed heterozygous amino acid changes at five positions—Leu424Val, Arg1017His, Val1114Ile, Ile1615Val, and Pro2238Gln—in both affected and normal monkeys. However, these missense variants did not segregate with the disease phenotype.

VMD2. The monkey *VMD2* gene consists of 11 exons, with its translation initiation codon in exon 2, as observed in its human orthologue. The complete cDNA was 2187 bp, encoding 585 amino acids. The *VMD2* gene encodes the bestrophin protein, which localizes to the basolateral plasma membrane of the RPE with the postulated function as an oligomeric chloride channel.[36,37] The hydropathy profile predicted that bestrophin contains four stretches of hydrophobic amino acids that function as transmembrane domains. Comparative sequence analysis demonstrated that monkey bestrophin had 19 amino acids different from its human homologue, and the four putative transmembrane domains are highly conserved. To date, 72 disease-associated nucleotide substitutions of the *VMD2* gene have been identified in patients with Best disease.[3,7,26] The mutation analysis of the *VMD2* gene in the monkey pedigree detected six amino acid sequence variants. A polymorphism (Val/Ile) was detected at codon 275 in the fourth transmembrane domain, which has also been reported in humans.[26] Four polymorphisms (Tyr465His, Thr542Met, Glu557Gln, and Thr566Ala) were detected in exon 10. These changes did not segregate with the disease. In addition, one nonsense mutation at codon 582 (Glu→Stop) in exon 11 was detected in two normal monkeys, whereas none of the examined six affected monkeys showed the change.

EFEMP1. The exon–intron gene structure of the monkey *EFEMP1* gene was also similar to the human *EFEMP1* gene. It was composed of 11 exons with its translation initiation codon in exon 2. The complete cDNA was 2034 bp, encoding 493 amino acids. Although the function of this gene remains unclear, this class of proteins is known to have characteristic sequence of repeated calcium-binding EGF-like domains.[4] The monkey *EFEMP1* cDNA was found to have six EGF repeats. Four EGF repeats (numbers 2–5) are encoded by single exons (exons 5–8), one EGF repeat (number 1) is encoded by three exons (exons 2–4), and EGF repeat number 6 is encoded by two exons (exons 9, 10). This finding is in agreement with one of the two transcriptional variants with a distinct 5′ untranslated region (UTR) described in its human homologue. Comparative sequence analysis demonstrated that the monkey *EFEMP1* has three amino acids different from that of the human, but the sequence in the entire region of six EGF repeats is completely conserved. In humans, a single mutation (Arg345Trp) that disrupts one of these domains is known to cause Malattia Leventinese.[4] No amino acid–changing polymorphisms were found in all the monkeys tested. Three single nucleotide polymorphisms (SNPs), that did not alter the amino acid sequence, were detected in exons 4, 5, and 10.

TIMP3. The monkey *TIMP3* gene consisted of five exons, similar to its human orthologue. The complete cDNA was 1887 bp in length, encoding 211 amino acids. *TIMP3* is the third member of the tissue inhibitors of metalloproteinase family, a group of zinc-binding endopeptidases involved in the degradation of the extracellular matrix. *TIMP3* has 12 cysteines characteristic of the TIMP family, which are proposed to form intramolecular disulfide bonds and tertiary structure for the functional properties of the mature protein. The predicted amino acid sequence of the monkey *TIMP3* gene was identical with the human orthologue, including the 12 cysteine residues. Mutations in the *TIMP3* gene are known to cause Sorsby's fundus dystrophy.[5] With a few exceptions,[38,39] most previously described mutations disrupt the disulfide bonds by changing residues into cysteines, leading to misfolding of the protein.[5,40] No coding sequence changes were detected in the *TIMP3* gene in monkeys by mutation screening.

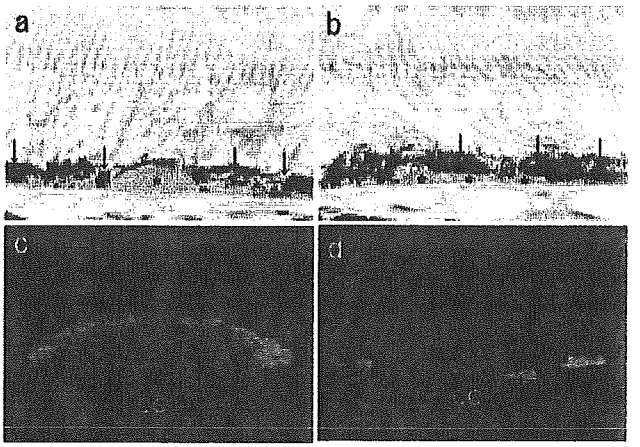

FIGURE 3. Drusen in the affected monkey retina. An affected 14-year-old male monkey (Fig. 1, monkey B). There were various-sized drusen, which were weakly stained by PAS (✱), between the RPE and choriocapillaris (CC) (**a**, **b**). These drusen were strongly reactive with antibodies against complement C5 (*green* channel). Lipofuscin autofluorescence is shown (*red*) in the RPE (**c**, **d**). Accumulation of lipofuscin in RPE cells was also obvious by PAS (**a**, **b**, *arrows*).

TABLE 4. Two-Point Lod Scores between the Monkey Macular Degeneration Locus and Markers at the Human Macular Degeneration Loci

Markers	Distance from the Gene (CM)	Order on the Chromosome (M)	Lod Scores at θ									Exclusion ($Z = -2$)
			0	0.001	0.005	0.01	0.05	0.1	0.2	0.3	0.4	
CORD8		154.28										
D1S431	10.5	165	$-\varepsilon$	−2.116	−1.422	−1.128	−0.483	−0.248	−0.071	−0.01	0.006	0.001
D1S2635	0	154.28	$-\varepsilon$	−11.078	−7.598	−6.112	−2.773	−1.469	−0.392	0.019	0.119	0.075
D1S2715	−6.9	147.01	$-\varepsilon$	−7.7	−4.925	−3.747	−1.162	−0.232	0.388	0.464	0.299	0.03
D1S498	−10.6	144.94	$-\varepsilon$	−1.124	−0.439	−0.154	0.416	0.564	0.567	0.433	0.227	0.0001
ABCA4		94.1										
D1S188	−2.3	91.7	$-\varepsilon$	−6.139	−4.058	−3.175	−1.24	−0.541	−0.05	0.074	0.066	0.01
D1S2849	−1.2	92.9	$-\varepsilon$	−1.766	−1.075	−0.784	−0.166	0.032	0.133	0.119	0.067	
D1S2868	0.1	94	$-\varepsilon$	−14.824	−10.623	−8.809	−4.599	−2.846	−1.264	−0.522	−0.146	0.1
STGD3		80.5										
D6S1662	−2.67	77.83	$-\varepsilon$	−1.232	−0.544	−0.257	0.324	0.476	0.472	0.34	0.17	0.0
D6S1048	0.28	80.78	$-\varepsilon$	−0.063	0.614	0.889	1.38	1.416	1.172	0.79	0.362	0.0
D6S1596	7.1	87.6	$-\varepsilon$	−8.746	−5.965	−4.78	−2.138	−1.127	−0.319	−0.025	0.049	0.05
D6S1609	12.08	92.58	$-\varepsilon$	−7.326	−5.235	−4.34	−2.302	−1.475	−0.724	−0.349	0.131	0.05
DHRD		56.1										
D2S2230	3.9	60	$-\varepsilon$	−11.691	−8.209	−6.719	−3.349	−2.006	−0.842	−0.325	−0.084	0.1
D2S378	1.1	57.2	$-\varepsilon$	−9.268	−6.482	−5.29	−2.593	−1.517	−0.588	−0.186	−0.019	0.05
ARMD1		192.2										
D1S384	−2.11	190.09	$-\varepsilon$	−5.565	−3.486	−2.606	−0.696	−0.032	0.375	0.389	0.236	0.01
D1S413	2.1	194.1	$-\varepsilon$	−11.068	−7.59	−6.106	−2.784	−1.501	−0.46	−0.067	0.047	0.05
D1S2622	3.7	195.9	$-\varepsilon$	−1.961	−1.271	−0.982	−0.375	−0.185	−0.084	−0.066	−0.047	0.0
VMD2		61.5										
D11S1993	−2.3	59.2	$-\varepsilon$	−1.615	−0.925	−0.636	−0.032	0.151	0.224	0.181	0.1	0.0
D11S4174	1.4	62.9	$-\varepsilon$	−7.132	−5.026	−4.112	−1.979	−1.102	−0.368	−0.087	0.003	0.01
D11S4076	7.3	66.8	$-\varepsilon$	−5.617	−3.537	−2.656	−0.736	−0.061	0.364	0.385	0.231	0.01
Rhodopsin		130.6										
D3S3515	−4.01	126.59	$-\varepsilon$	−2.756	−1.379	−0.803	0.383	0.717	0.775	0.584	0.302	0.001
D3S3720	−2.8	127.8	$-\varepsilon$	−2.626	−1.247	−0.67	0.531	0.879	0.945	0.729	0.389	0.001
D3S1269	0.3	130.9	$-\varepsilon$	−11.566	−8.081	−6.588	−3.2	−1.846	−0.7	−0.238	−0.062	0.05
Timp3		31.5										
D22S1162	7.05	38.55	$-\varepsilon$	−3.587	−2.203	−1.619	−0.365	0.055	0.291	0.276	0.159	0.005
D22S280	0	31.5	$-\varepsilon$	−4.051	−2.664	−2.075	−0.785	−0.321	−0.002	0.065	0.044	0.01
D22S273	−1	30.5	$-\varepsilon$	−1.878	−1.187	−0.896	−0.278	−0.078	0.026	0.025	0.004	0.0
CTRP5		118.7										
D11S4127	−1.6	117.1	$-\varepsilon$	−0.771	−0.088	0.192	0.73	0.827	0.719	0.495	0.244	0.0
D11S924	0.2	118.9	$-\varepsilon$	−1.424	−0.736	−0.449	0.137	0.298	0.322	0.232	0.113	0.0
D11S4129	4.18	121.58	$-\varepsilon$	−9.057	−6.275	−5.089	−2.435	−1.41	−0.566	−0.214	−0.054	0.05
STGD4		26.1										
D4S403	0	26.1	$-\varepsilon$	−16.798	−11.919	−9.83	−5.081	−3.159	−1.445	−0.633	−0.206	0.1
D4S391	1.2	27.3	$-\varepsilon$	−3.615	−2.231	−1.647	−0.392	0.026	0.255	0.234	0.13	0.005
CORD5	(Interval)	64.5										
D17S938	0	64.5	$-\varepsilon$	−16.296	−11.422	−9.339	−4.638	−2.776	−1.176	−0.466	−0.125	0.1
D17S796	0	64.5	$-\varepsilon$	−3.594	−2.209	−1.624	−0.358	0.075	0.324	0.305	0.176	0.0
MCDR1	(Interval)	98.1										
D6S434	4.3	102.4	$-\varepsilon$	−4.496	−3.103	−2.507	−1.163	−0.632	−0.183	−0.005	0.043	0.0
CORD9	(Interval)	47.6										
D8S1820	0	47.6	$-\varepsilon$	−11.981	−8.501	−7.014	−3.65	−2.277	−1.002	−0.385	−0.092	0.1

ELOVL4. We have reported cloning and characterization of the *ELOVL4* gene in the cynomolgus monkey.[11] Three mutations leading to truncation of the *ELOVL4* protein were reported in humans with Stargardt-like macular dystrophy[23,42] (Karen G, et al. *IOVS* 2004;45:ARVO E-Abstract 1766). Mutation analysis of monkeys with macular degeneration did not detect any amino acid–altering sequence changes. Silent polymorphisms were observed in exons 1, 3, and 4 of the *ELOVL4* gene.

Linkage Analysis of Candidate Gene Loci

The methodology we used to screen for mutations in the candidate genes could miss disease-associated changes that may be present in the promoter or intronic regions; therefore, linkage analysis was performed to exclude the five genes further. Moreover, the macular degeneration phenotype in the monkey pedigree could be caused by a single gene defect. In these cases, linkage analysis would be a comprehensive approach to confirm or exclude a particular gene locus. Microsatellite markers linked to the five candidate gene loci in addition to eight human macular degeneration loci—*ABCA4*, *VMD2*, *DHRD* (*EFEMP1*), *TIMP3*, *STGD3* (*ELOVL4*), Cone rod dystrophy-8 (*CORD-8*), age-related macular degeneration 1 (*ARMD1*, gene Hemicentin1), rhodopsin, *STGD4*, North Carolina macular degeneration (*MCDR1*), *CORD9*, late-onset retinal degeneration (*CTRP5*), and *CORD5* loci—were analyzed to test for linkage with the macular degeneration in the monkey pedigree. None of the tested loci gave significant positive lod scores (Table 4). We also constructed haplotypes using the genotype data of markers at the 13 loci. This analysis further supported the exclusion of these loci from being among those that might harbor the gene associated with macular degeneration in these monkeys.

Discussion

We report a detailed description of early-onset macular degeneration in cynomolgus monkeys and the exclusion of known genes responsible for macular degeneration in humans as a disease-associated gene in this animal model. Several forms of macular degeneration have been described in humans, including autosomal dominant, autosomal recessive, and X-linked modes of inheritance. The most common form of macular disease in humans is AMD. Major clinical characteristics of AMD are loss of central vision with RPE atrophy or exudation. The presence of subretinal deposits known as drusen is one of the early signs observed in AMD and several other macular degenerations. Recent studies suggest that the process of drusen formation includes inflammatory and immune-mediated events.[35] Immunohistochemical examinations have revealed that drusen contains activated complement factors. These molecules include C5, the cleavage product of C3 (C3b, iC3b, and C3dg), and the terminal complement complex C5b-9. Clinical and histologic studies of the affected monkeys showed the presence of drusen (Figs. 2, 3). Immunologic analysis demonstrated that drusen in monkeys had C5 as a component, suggesting that the nature of monkey drusen was similar to that reported in human AMD. At the same time, the onset of the disease in monkeys is at ~2 years of age; therefore, the monkey macular degeneration resembles early-onset human macular degeneration with drusen.

Comparison of the gene maps and chromosome painting data revealed a high degree of synteny and genome conservation between human and Macaque genomes.[43,44] Amplification of cynomolgus monkey DNA with human microsatellite marker primers and sequence analysis revealed that not only the sequences flanking the microsatellite repeat regions but also the polymorphic nature of these repeats is conserved between human and monkey genomes (data not shown). Comparative studies on human and chimpanzee genomes have shown the same average heterozygosity at microsatellite marker loci and conserved genetic distance between markers.[45] Molecular cloning of monkey orthologues of the human *ABCA4*, *VMD2*, *EFEMP1*, *TIMP3*, and *ELOVL4* genes further demonstrated the high conservation between the human and macaque genomes not only in the organization of the gene structure, but also at the sequence level. Considering the high conservation between human and macaque genomes, human macular degeneration loci can be considered plausible candidates for identification of the gene associated with macular degeneration in the monkeys. We tested this hypothesis using microsatellite markers linked to human macular degeneration loci and successfully amplified microsatellites in the monkey DNA with human primers. However, we failed to establish linkage with the tested loci, and the subsequent haplotype analysis further confirmed this finding. Therefore, the macular degeneration locus in the monkey pedigree is not likely to be associated with the regions of the monkey genome that are syntenic to human genomic regions comprising the 13 macular disease loci tested. Mutation analysis of candidate genes also supported the exclusion of the *ABCA4*, *VMD2*, *EFEMP1*, *TIMP3*, and *ELOVL4* genes. The analyses detected five- and six-amino-acid substitutions in the *ABCA4* and *VMD2* genes, respectively. Some silent nucleotide substitutions or intronic sequences changes, such as small insertions/deletions, SNPs, and variations of short tandem repeats were observed in the *EFEMP1*, *TIMP3*, and *ELOVL4* genes. All these sequence variants did not segregate with the disease phenotype in the extended pedigree. Hence, these changes were interpreted as benign polymorphisms.

In the *ABCA4* sequence of a normal monkey, we found two amino acid replacements (K223Q and R1300Q) that are associated with Stargardt disease in humans. Because of the extensive conservation between the monkey and human gene sequences, one would expect these amino acid changes to have similar disease-associated effects in monkeys. One explanation of this discrepancy could be that K223Q and R1300Q are not causing the disease phenotype in humans, but rather represent markers linked to disease-causing mutations somewhere else in the gene. Alternatively, the disease-causing effect of these amino acid changes on the function of the human ABCA4 protein could be eliminated or compensated for by other differences in the monkey protein. Comparative analysis of the monkey and human genes may provide clues for understanding the molecular pathogenesis caused by *ABCA4* variation. In the *VMD2* gene sequence of normal monkeys, we found a nonsense mutation at codon 582. The change is located at the fourth residue from the C terminus. Bestrophin was shown to form oligomeric chloride channels in cell membranes.[37] The C-terminal cytosolic tail, encoded by exons 10 and 11, has been reported not to be essential for the protein's function. Moreover, although 72 nucleotide substitutions have been identified in Best disease to date,[3,7,26] none of them is reported in exons 10 and 11. Hence, the deletion of four amino acids from the C-terminal end of the protein could be considered not to be associated with the disease.

In summary, we demonstrated that none of the 13 human macular degeneration loci tested were involved in causing the macular degeneration phenotype observed in the monkey pedigree. These results demonstrate the need for additional studies to identify the genetic locus associated with the phenotype in these monkeys and to understand the genetic defect underlying the disease. Identification of the gene responsible for this specific macular degeneration phenotype not only defines a new candidate locus for human macular degeneration, but also provides a primate animal model that can be extensively studied for elucidation of the mechanisms, diagnosis, prophylaxis, and treatment of macular degenerations, including AMD.

References

1. Michaelides M, Hunt DM, Moore AT. The genetics of inherited macular dystrophies. *J Med Genet*. 2003;9:641–650.
2. Allikmets R, Singh N, Sun H, et al. A photoreceptor cell-specific ATP-binding transporter gene (ABCR) is mutated in recessive Stargardt macular dystrophy. *Nat Genet*. 1997;3:236–246.
3. Petrukhin K, Koisti MJ, Bakall B, et al. Identification of the gene responsible for Best macular dystrophy. *Nat Genet*. 1998;3:241–247.
4. Stone EM, Lotery AJ, Munier FL, et al. A single EFEMP1 mutation associated with both Malattia Leventinese and Doyne honeycomb retinal dystrophy. *Nat Genet*. 1999;2:199–202.
5. Weber BH, Vogt G, Pruett RC, Stohr H, Felbor U. Mutations in the tissue inhibitor of metalloproteinases-3 (TIMP3) in patients with Sorsby's fundus dystrophy. *Nat Genet*. 1994;4:352–356.
6. Zhang K, Kniazeva M, Han M, et al. A 5-bp deletion in ELOVL4 is associated with two related forms of autosomal dominant macular dystrophy. *Nat Genet*. 2001;1:89–93.
7. Marquardt A, Stohr H, Passmore LA, et al. Mutations in a novel gene, VMD2, encoding a protein of unknown properties cause juvenile-onset vitelliform macular dystrophy (Best's disease). *Hum Mol Genet*. 1998;9:1517–1525.
8. Bernstein PS, Tammur J, Singh N, et al. Diverse macular dystrophy phenotype caused by a novel complex mutation in the *ELOVL4* gene. *Invest Ophthalmol Vis Sci*. 2001;13:3331–3336.
9. Dithmar S, Curcio CA, Le NA, Brown S, Grossniklaus HE. Ultrastructural changes in Bruch's membrane of apolipoprotein E-deficient mice. *Invest Ophthalmol Vis Sci*. 2000;8:2035–2042.
10. Mata NL, Tzekov RT, Liu X, et al. Delayed dark-adaptation and lipofuscin accumulation in abcr+/− mice: implications for involvement of ABCR in age-related macular degeneration. *Invest Ophthalmol Vis Sci*. 2001;8:1685–1690.

11. Rakoczy PE, Zhang D, Robertson T, et al. Progressive age-related changes similar to age-related macular degeneration in a transgenic mouse model. *Am J Pathol.* 2002;4:1515–1524.
12. Stafford TJ. Maculopathy in an elderly sub-human primate. *Mod Probl Ophthalmol.* 1974;0:214–219.
13. El-Mofty A, Gouras P, Eisner G, Balazs EA. Macular degeneration in rhesus monkey (Macaca mulatta). *Exp Eye Res.* 1978;4:499–502.
14. Hope GM, Dawson WW, Engel HM, et al. A primate model for age related macular drusen. *Br J Ophthalmol.* 1992;1:11–16.
15. Nicolas MG, Fujiki K, Murayama K, et al. Studies on the mechanism of early onset macular degeneration in cynomolgus monkeys. II. Suppression of metallothionein synthesis in the retina in oxidative stress. *Exp Eye Res.* 1996;4:399–408.
16. Nicolas MG, Fujiki K, Murayama K, et al. Studies on the mechanism of early onset macular degeneration in cynomolgus (Macaca fascicularis) monkeys. I. Abnormal concentrations of two proteins in the retina. *Exp Eye Res.* 1996;3:211–219.
17. Suzuki MT, Terao K, Yoshikawa Y. Familial early onset macular degeneration in cynomolgus monkeys (Macaca fascicularis). *Primates.* 2003;3:291–294.
18. Klaver CC, Wolfs RC, Assink JJ, et al. Genetic risk of age-related maculopathy: population-based familial aggregation study. *Arch Ophthalmol.* 1998;12:1646–1651.
19. Seddon JM, Ajani UA, Mitchell BD. Familial aggregation of age-related maculopathy. *Am J Ophthalmol.* 1997;2:199–206.
20. Meyers SM, Greene T, Gutman FA. A twin study of age-related macular degeneration. *Am J Ophthalmol.* 1995;6:757–766.
21. Tuo J, Bojanowski CM, Chan CC. Genetic factors of age-related macular degeneration. *Prog Retin Eye Res.* 2004;2:229–249.
22. Abecasis GR, Yashar BM, Zhao Y, et al. Age-related macular degeneration: a high-resolution genome scan for susceptibility loci in a population enriched for late-stage disease. *Am J Hum Genet.* 2004;3:482–494.
23. Ayyagari R, Zhang K, Hutchinson A, et al. Evaluation of the ELOVL4 gene in patients with age-related macular degeneration. *Ophthalmic Genet.* 2001;4:233–239.
24. Allikmets R. Further evidence for an association of ABCR alleles with age-related macular degeneration: the International ABCR Screening Consortium. *Am J Hum Genet.* 2000;2:487–491.
25. Felbor U, Doepner D, Schneider U, Zrenner E, Weber BH. Evaluation of the gene encoding the tissue inhibitor of metalloproteinases-3 in various maculopathies. *Invest Ophthalmol Vis Sci.* 1997; 6:1054–1059.
26. Lotery AJ, Munier FL, Fishman GA, et al. Allelic variation in the VMD2 gene in best disease and age-related macular degeneration. *Invest Ophthalmol Vis Sci.* 2000;6:1291–1296.
27. Honjo S. The Japanese Tsukuba Primate Center for Medical Science (TPC): an outline. *J Med Primatol.* 1985;2:75–89.
28. Marmor MF, Zrenner E. Standard for clinical electroretinography (1999 update): International Society for Clinical Electrophysiology of Vision. *Doc Ophthalmol.* 1998;2:143–156.
29. Dockhorn-Dworniczak B, Dworniczak B, Brommelkamp L, et al. Non-isotopic detection of single strand conformation polymorphism (PCR-SSCP): a rapid and sensitive technique in diagnosis of phenylketonuria. *Nucleic Acids Res.* 1991;9:2500.
30. Liu W, Smith DI, Rechtzigel KJ, Thibodeau SN, James CD. Denaturing high performance liquid chromatography (DHPLC) used in the detection of germline and somatic mutations. *Nucleic Acids Res.* 1998;6:1396–1400.
31. Griesinger IB, Sieving PA, Ayyagari R. Autosomal dominant macular atrophy at 6q14 excludes CORD7 and MCDR1/PBCRA loci. *Invest Ophthalmol Vis Sci.* 2000;1:248–255.
32. Terwilliger JD, Ott J. *Handbook of Human Genetic Linkage.* Baltimore, MD: The Johns Hopkins University Press; 1994.
33. Otto J. *Analysis of Human Genetic Linkage.* Baltimore, MD: The Johns Hopkins University Press; 1999.
34. Khani SC, Karoukis AJ, Young JE, et al. Late-onset autosomal dominant macular dystrophy with choroidal neovascularization and nonexudative maculopathy associated with mutation in the RDS gene. *Invest Ophthalmol Vis Sci.* 2003;8:3570–3577.
35. Mullins RF, Russell SR, Anderson DH, and Hageman GS. Drusen associated with aging and age-related macular degeneration contain proteins common to extracellular deposits associated with atherosclerosis, elastosis, amyloidosis, and dense deposit disease. *FASEB J.* 2000;7:835–846.
36. Marmorstein AD, Marmorstein LY, Rayborn M, et al. Bestrophin, the product of the Best vitelliform macular dystrophy gene (VMD2), localizes to the basolateral plasma membrane of the retinal pigment epithelium. *Proc Natl Acad Sci USA.* 2000;23: 12758–12763.
37. Sun H, Tsunenari T, Yau KW, Nathans J. The vitelliform macular dystrophy protein defines a new family of chloride channels. *Proc Natl Acad Sci USA.* 2002;6:4008–4013.
38. Tabata Y, Isashiki Y, Kamimura K, Nakao K, Ohba N. A novel splice site mutation in the tissue inhibitor of the metalloproteinases-3 gene in Sorsby's fundus dystrophy with unusual clinical features. *Hum Genet.* 1998;2:179–182.
39. Langton KP, McKie N, Curtis A, et al. A novel tissue inhibitor of metalloproteinases-3 mutation reveals a common molecular phenotype in Sorsby's fundus dystrophy. *J Biol Chem.* 2000;35: 27027–27031.
40. Felbor U, Stohr H, Amann T, Schonherr U, Weber BH. A novel Ser156Cys mutation in the tissue inhibitor of metalloproteinases-3 (TIMP3) in Sorsby's fundus dystrophy with unusual clinical features. *Hum Mol Genet.* 1995;12:2415–2416.
41. Umeda S, Ayyagari R, Suzuki MT, et al. Molecular cloning of ELOVL4 gene from cynomolgus monkey (Macaca fascicularis). *Exp Anim.* 2003;2:129–135.
42. Edwards AO, Donoso LA, Ritter R III. A novel gene for autosomal dominant Stargardt-like macular dystrophy with homology to the SUR4 protein family. *Invest Ophthalmol Vis Sci.* 2001;11:2652–2663.
43. Wienberg J, Stanyon R. Comparative painting of mammalian chromosomes. *Curr Opin Genet Dev.* 1997;6:784–791.
44. O'Brien SJ, Menotti-Raymond M, Murphy WJ, et al. The promise of comparative genomics in mammals. *Science.* 1999;5439:458–462,479–481.
45. Crouau-Roy B, Service S, Slatkin M, Freimer N. A fine-scale comparison of the human and chimpanzee genomes: linkage, linkage disequilibrium and sequence analysis. *Hum Mol Genet.* 1996;8: 1131–1137.

Available online at www.sciencedirect.com
SCIENCE DIRECT®
Molecular Genetics and Metabolism 82 (2004) 173–179
Molecular Genetics and Metabolism
www.elsevier.com/locate/ymgme

Genitourinary phenotype in XX patients with distal 9p monosomy

Yoko Fujimoto,[a,b,c] Torayuki Okuyama,[d] Makoto Iijima,[e] Toshiaki Tanaka,[f] Reiko Horikawa,[c] Koichiro Yamada,[b] and Tsutomu Ogata[a,*]

[a] *Department of Endocrinology and Metabolism, National Research Institute for Child Health and Development, Tokyo, Japan*
[b] *Department of Pediatrics, Shouwa University School of Medicine Fujigaoka Hospital, Yokohama, Japan*
[c] *Division of Adolescent and Young Adult Medicine, National Center for Child Health and Development, Tokyo, Japan*
[d] *Division of Clinical Genetics and Molecular Medicine, National Center for Child Health and Development, Tokyo, Japan*
[e] *Division of Nephrology, National Center for Child Health and Development, Tokyo, Japan*
[f] *Division of Endocrinology and Metabolism, National Center for Child Health and Development, Tokyo, Japan*

Received 30 January 2004; received in revised form 5 April 2004; accepted 5 April 2004
Available online 8 May 2004

Abstract

Although testicular development has been shown to be variably impaired in XY patients with distal 9p monosomy, ovarian and other genitourinary phenotype has poorly been studied in XX patients monosomic for the distal 9p region. Thus, we studied a 13-month-old infant with 46,XX,der(9)t(9;10)(p23;p13) (case 1) and an 11-year-old girl with 46,XX,der(9)t(9;16)(p23;q22) (case 2). Case 1 had primary hypogonadism (basal serum follicle stimulating hormone [FSH], 40.0 mIU/mL; leteinizing hormone [LH], 1.2 mIU/mL; estradiol [E_2], <10 pg/mL), whereas case 2 had age-appropriate pubertal development (breast, Tanner stage 4; pubic hair, Tanner stage 3; menarche 11.7 years of age) and hormone values (FSH, 7.3 mIU/mL; LH, 6.7 mIU/mL; E_2, 47 pg/mL). In addition, case 1 had hypoplastic labia majora, short distance between the vaginal orifice and the anus, and five renal cysts, and case 2 had anal atresia, short distance between the vaginal orifice and the anus, bilateral hydronephrosis of grade 3 with probable ureteropelvic junction stenosis, and renal dysfunction (serum creatinine, 1.52 mg/dL; urea nitrogen, 34.5 mg/dL). Fluorescence in situ hybridization analysis for five regions and microsatellite analysis for 10 loci on 9p confirmed hemizygosity for the distal 9p region with the breakpoints between *IFNA* and *D9S285* in case 1 and between *D9S168* and *D9S286* in case 2. The results, in conjunction with the previous data in XX patients with molecularly defined distal 9p monosomy, are consistent with the presence of a gene(s) involved in the development of indifferent gonad or subsequent ovarian differentiation in a ~11 Mb region distal to *D9S168*. In addition, it is possible that a gene(s) for anoperineal and renal development also maps distal to *D9S168* and that for external genital development maps distal to *D9S285* at the position ~16 Mb from the 9p telomere.
© 2004 Elsevier Inc. All rights reserved.

Keywords: 9p monosomy; Sex determination; Ovarian development; Genitourinary development; Penetrance

Introduction

Testicular development has been shown to be variable from nearly normal testis formation to nearly complete gonadal dysgenesis or agenesis in XY patients with distal 9p monosomy [1–3]. Since the degree of impaired testis development is independent of the deletion size, it has been suggested that a gene(s) for testis development resides in the 9p monosomic region shared by the patients with defective testis development, and that haploinsufficiency of the gene(s) leads to various degrees of impaired testis formation [1–3]. Although the gene(s) for testis development has not been identified, it has has been localized to a terminal ~700 kb region distal to the exons of *DMRT1* (doublesex and mab-3 related transcription factor 1), on the basis of molecular studies in XY sex reversed patients with distal 9p monosomy [2]. The relevance of epigenetic imprinting is unlikely, because impaired male sex development can occur regardless of the parental origin of deleted 9p chromosomes [3].

* Corresponding author. Fax: +81-3-5431-6057.
E-mail address: tomogata@nch.go.jp (T. Ogata).

1096-7192/$ - see front matter © 2004 Elsevier Inc. All rights reserved.
doi:10.1016/j.ymgme.2004.04.003

However, ovarian phenotype has poorly been studied in XX patients hemizygous for the distal 9p region. In addition, other genitourinary findings have also poorly been examined in patients with distal 9p monosomy. Here, we report on two Japanese XX patients monosomic for the distal 9p region, and discuss on ovarian and other genitourinary development in distal 9p monosomy.

Case reports

Case 1

This female infant was the 2.92 kg (−0.5 SD) product of an uncomplicated term pregnancy. The parents were non-consanguineous and healthy. Shortly after birth, she was referred to our hospital because of multiple minor anomalies. Physical examination showed a feeble and hypopigmented infant with various dysmorphic features indicative of 9p monosomy syndrome, such as trigonocephaly, up-slanting palpebral fissures, flat nasal ridge, small and deformed ears, high arched palate, micrognathia, and bilateral short second and third fingers. External genitalia were feminized with hypoplastic labia majora. The distance between the vaginal orifice and the anus appeared to be diminished. There were no major anomalies. Thereafter, she had developmental retardation: she controlled her head at 6 months of age and sat without support at 12 months of age.

At 13 months of age, she was evaluated for genitourinary development. Biochemical studies indicated primary hypogonadism (Table 1) and normal renal function with serum creatinine of 0.29 mg/dL (age-matched normal range, 0.3–0.6 mg/dL) and urea nitrogen of 10.0 mg/dL (7.4–19.1 mg/dL) [6]. Abdominal ultrasound examinations showed rudimentary uterus and failed to detect gonadal structures. Renal size was normal (the maximum renal length, 7.3 cm for the right kidney and 7.2 cm for the left kidney) (height-matched reference data, 5.2–7.8 cm) [9] as was renal echogenicity, but five simple cysts of 3–6 mm in diameter were detected in the right renal cortex. At present, she is 17 months old, measures 79.1 cm (+0.2 SD), and weighs 9.35 kg (−0.5 SD).

Case 2

This girl was a cousin of the previously reported female infant with 46,XX,der(9)t(9;16)(p23;q22) (case 3 in Table 1) [3]; the father of case 2 was the younger brother of the father of case 3 who had 46,XY,t(9;16)(p23;q22). The parents of case 2 were non-consanguineous and healthy, as were the parents of case 3. Case 2 was also found to have chromosomal abnormality involving 9p at another hospital.

At $11\frac{2}{12}$ years of age, she came to our hospital with her mother, asking appropriate examination and management. Allegedly, she had anal atresia that was surgically treated at four months of age, cleft palate that was repaired at 6 months of age, and sensory deafness that was diagnosed by auditory brainstem response at 18 months of age. She was repeatedly affected with intractable otitis media that often required hospitalization, and routine laboratory tests at the time of admissions indicated gradual increase in serum creatinine level from ~6 years of age. She had severe developmental retardation and attended a special school for mentally delayed children.

Physical examination revealed various minor anomalies consistent with 9p monosomy syndrome, such as trigonocephaly, up-slanting palpebral fissures, large nose, flat nasal ridge, short anteverted nostrils, long philtrum, high arched palate, and distal symphalangism of the bilateral 2nd–5th fingers. External genitalia were those of normal girls, and the distance between the vaginal orifice and the anus appeared to be shortened. She exhibited breast development at Tanner stage 3 and pubic hair development at Tanner stage 2 (Japanese reference data: breast stage 3, 11.6 ± 1.5 years; pubic hair stage 2, 11.7 ± 1.6) [8]. Biochemical studies indicated normal pituitary-gonadal function (Table 1), and impaired renal function with increased serum creatinine of 1.52 mg/dL (0.4–0.8 mg/dL), urea nitrogen of 34.5 mg/dL (6.9–18.5 mg/dL), and uric acid of 8.0 mg/dL (2.5–6.0 mg/dL) [6]. Abdominal ultrasound examinations delineated moderately enlarged uterus and ovary-like structures. Renal size was normal (the maximum renal length, 7.5 cm for the right kidney, and 7.2 cm for the left kidney) (height-matched normal range, 7.0–9.6 cm) [9], but hydronephrosis of grade 3 with probable ureteropelvic junction stenosis was delineated bilaterally. Furthermore, the echogenicity was stronger in the renal cortex that in the liver, suggesting renal dysplasia. Thus, periodical examinations were recommended.

At 11.7 years of age, she experienced menarche, and exhibited breast development at Tanner stage 4 and pubic hair development at Tanner stage 3 (Japanese reference data: menarche, 12.25 ± 1.25 years; breast stage 4, 13.3 ± 1.5 years; pubic hair stage 3, no data) [8]. At present, she is $11\frac{9}{12}$ years old, measures 123.1 cm (−4.3 SD), and weighs 28.4 kg (−1.5 SD).

Methods

Conventional and molecular cytogenetic studies

After obtaining written informed consent, peripheral blood was obtained from case 1 and her parents and from case 2. Chromosome analysis was performed on 50 peripheral lymphocytes with G-banding. Fluorescence in situ hybridization (FISH) analysis was carried out for lymphocyte metaphase spreads, with a bacterial artificial chromosome (BAC) probe containing the marker *305J7-T7* (41-L13), a yeast artificial chromosome (YAC) probe

Table 1
Ovariand and other genitourinary findings in karyotypic female patients with molecularly defined distal 9p monosomy

Case	Age (y:m)	E_2[a] (pg/mL)	FSH[a] (mIU/mL)	LH[a] (mIU/mL)	Tanner stage	Menarche (years)	Fertility	Gonadal histology	Müllerian derivatives	External genitalia	Anoperineal region	Renal region
1	1:02	<10 (<10)	40.0 (1.6–5.7)	1.2 (<1.0)	B1, P1	—	—	N.E.	Uterus	Hypoplastic labia majora	Short A–V length	Cystic lesions ($n = 5$)
2	11:08	47 (<10–120)	7.3 (1.1–8.7)	6.7 (0.3–8.1)	B4, P3	11.7 (12.25 ± 1.25)	—	N.E.	Uterus	Normal	Anal atresia short A–V length	Hydronephrosis renal dysfunction
3[b]	1:05	12 (<20)	41.0 (1.6–5.7)	2.0 (<1.0)	B1, P1	—	—	N.E.	Uterus	Normal	Anal atresia	Normal
	5:09	<10 (<10)	17.1 (0.3–3.8)	0.7 (<1.0)	B1, P1							
4	2:04	<10 (<10)	7.6 (1.6–5.7) Peak, 38.2[e] (2.2–16.4)	0.6 (<1.0) Peak, 9.4[e] (2.6–4.7)	B1, P1	—	—	N.E.	Uterus	Normal	Normal	Normal
5[c]	11:08	43 (<10–130)	7.2 (1.5–6.0)	3.9 (0.1–2.5)	B4, P2	10.8 (12.25 ± 1.25)	—	N.E.	Uterus	Hypoplastic labia majora	Normal	Normal
6	Fetus (24 weeks)	—	—	—	—	—	—	Normal	Normal	Normal	Normal	Normal
7[d]	Adult	N.E.	N.E.	N.E.	N.E.	N.E.	Yes	N.E.	N.E.	N.E.	N.E.	N.E.

References: cases 1 and 2 (this report); case 3, Muroya et al. [3] (case 6 in [3]); cases 4 and 5, Ogata et al. [4] (cases 2 and 1 in [4], respectively); case 6, Vialard et al. [5]; and case 7, Calvari et al. [2].
E_2: estradiol, FSH: follicle stimulating hormone; LH: luteinizing hormone; B: breast; P: pubic hair; N.E.: not examined; and A–V: the anus to the vaginal orifice.
The values in parentheses for Japanese cases 1–5 represent age- and sex-matched Japanese reference data [6–8].
[a] Basal serum hormone values.
[b] The cousin of case 2; case 3 has been reported at $1\frac{5}{12}$ years of age, and endocrine data obtained at $5\frac{9}{12}$ years of age are also shown.
[c] Case 5 has been described at $8\frac{1}{12}$ years of age, and the latest unpublished data are shown in this Table.
[d] Case 7 has produced two 46,XY sex reversed patients with a submicroscopic distal 9p monosomy.
[e] Peak values in a gonadotropin releasing homone test (100 μg/m^2 bolus i.v.; blood sampling at 0, 30, 60, 90, and 120 min).

containing *D9S1779* (757A1), a YAC probe containing *D9S1858* (765H2), a BAC probe containing *DMRT1* (DMRT1/BAC), and a P1 phage artificial chromosome (PAC) probe containing *D9S1136* (34H2), together with a BAC probe for *APBA1* at 9q13–21 used as an internal signal control [3,10–12]. The probe for *APBA1* was labeled with biotin and detected by avidin conjugated to fluorescein isothiocyanate, and the remaining probes were labeled with digoxigenin and detected by rhodamine anti-digoxigenin.

Microsatellite analysis

Leukocyte genomic DNA of case 1 and her parents and of case 2 was amplified by polymerase chain reaction (PCR) with fluorescently labeled forward primers and unlabeled reverse primers defining 10 loci on 9p (Table 2). The primer sequences and the PCR conditions were as described in Genome Database (http://www.gdb.org). The PCR products were determined for the fragment size on an autosequencer (ABI PRISM 310), using GeneScan software 2.1. In addition, leukocyte genomic DNA of the cousin of case 2 (case 3 in Table 1) and the uncle of case 2 (the father of case 3), that had been collected previously [3], was similarly analyzed with permission.

Results

Conventional and molecular cytogenetic studies

The karyotype was 46,XX,der(9)t(9;10)(p23;p13) in case 1, 46,XX,t(9;10)(p23;p13) in her mother, and 46,XY in her father. Case 2 had a 46,XX,der(9)t(9;16)(p23;q22) karyotype, as did her cousin (case 3).

Representative FISH results are shown in Fig. 1A, and the data are summarized in Table 2. The 9p regions defined by the five probes were deleted from the abnormal chromosome 9 and preserved on the normal chromosome 9 in cases 1 and 2. In the mother of case 1, the corresponding regions were identified on the der(10) chromosome as well as on the normal chromosome 9, thereby confirming the translocation. The data of the cousin and the uncle of case 2 were based on the previous studies [3].

Microsatellite analysis

Representative results are shown in Fig. 1B, and the data are summarized in Table 2. In case 1, maternal alleles for *D9S1779*, *D9S288*, and *D9S285* were not inherited by the patient, while paternal alleles for the three loci were transmitted to the patient. For *IFNA*, *D9S169*, and *D9S165*, both maternal and paternal alleles were transmitted to the patient. Thus, it was shown that the abnormal chromosome 9 of cases 1 was of maternal origin and missing a distal 9p region with the breakpoint between *IFNA* and *D9S285*.

In case 2, two alleles were detected for *D9S168*, *D9S169*, and *D9S165*, and single alleles only were identified for the remaining seven loci. No allele common to the patient and her cousin was identified for *D9S1779* and *D9S288*. The cousin of case 2 did not inherit paternal alleles for *D9S288* and *D9S286*. Collectively, since the 9p breakpoint should be identical between case 2 and her cousin, it was determined to

Table 2
The results of FISH and microsatellite analysis

Locus/region	Chromosoma location	Methods	Case 1			Case 2		
			Father	Patient	Mother	Patient	Cousin[a]	Uncle[a,b]
41-L13/BAC	9p24.3	FISH	Two copies	Single copy	Two copies[c]	Single copy	Single copy	Two copies[c]
D9S1779	9p24.3	MS	121, 123	123	143, 145	135[c]	141	137, 141
757A1/YAC	9p24.3	FISH	Two copies	Single copy	Two copies[c]	Single copy	Single copy	Two copies[c]
765H2/YAC	9p24.3	FISH	Two copies	Single copy	Two copies[c]	Single copy	Single copy	Two copies[c]
DMRT1/BAC	9p24.3	FISH	Two copies	Single copy	Two copies[c]	Single copy	Single copy	Two copies[c]
D9S129	9p24.3	MS	128	128	128, 130	130	130	128, 130
34H2/PAC	9p24.3–p24.1	FISH	Two copies	Single copy	Two copies[c]	Single copy	Single copy	Two copies[c]
D9S1871	9p24.3–p24.1	MS	140, 142	142	140, 142	142	142	142, 148
D9S288	9p24.3–p24.1	MS	120, 134	134	120, 124	140[d]	124	128, 130
D9S286	9p23	MS	153, 155	153	153	157[d]	157	153, 155
D9S168	9p23	MS	232	232	226, 232	226, 236	226	226, 232
D9S285	9p22	MS	120	120	104, 118	120	120	112, 120
IFNA	9p22	MS	141, 147	143, 147	143, 149	147	141, 147	141, 147
D9S169	9p21.1	MS	267	257, 267	257, 261	261, 267	261, 263	257, 261
D9S165	9p21.1	MS	212	212, 218	208, 218	211, 215	207, 211	211, 213

BAC: bacterial artificial chromosome; YAC: yeast artificial chromosome; PAC: P1 phage artificial chromosome; FISH: fluorescence in situ hybridization analysis; and MS: microsatellite analysis. The locus/region order and the chromosomal location are based on the previous reports [2,13,14]. The Arabic numbers for microsatellite analysis indicate the sizes of fragments produced by polymerase chain reaction (bp).

[a] The microsatellite results are obtained in this study, and the FISH data are based on the previous report [3].

[b] The father of the cousin.

[c] One signal on the normal chromosome 9, and the other signal on the translocated chromosome involving the distal 9p.

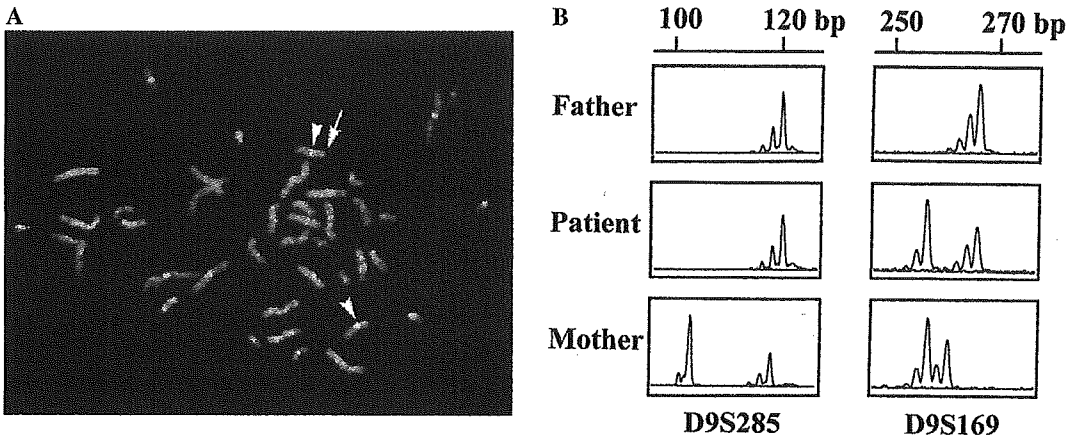

Fig. 1. (A) Representative FISH analysis in case 1. Only a single signal is detected for *DMRT1* (arrows), whereas two signals are found for *APBA1* used as an internal signal control (arrowheads). (B) Representative microsatellite results in case 1. For *D9S285*, the paternal allele only is transmitted to the patient and the maternal alleles are not inherited by the patient, demonstrating hemizygosity of this locus in the patient. For *D9S169*, the patient is heterozygous with the paternally and maternally derived alleles.

reside between *D9S168* and *D9S286* in case 2 and her cousin.

Discussion

Ovarian and other genitourinary development was different between cases 1 and 2 with molecularly confirmed distal 9p monosomy. Case 1 had hypergonadotropic hypogonadism consistent with ovarian dysfunction, together with external genital, anoperineal, and renal lesions. Case 2 had menarche and age-appropriate pubertal development indicative of normal ovarian function, and manifested anoperineal and renal lesions. The FSH dominant hypergonadotropinism in case 1 would primarily be due to her young age, because primary ovarian dysfunction is usually manifested by FSH dominant hypergonadotropinism in prepubertal girls and by elevation of both FSH and LH in pubertal to adult females [15,16]. Thus, although the effects of extra chromosomal materials translocated onto distal 9p can not be excluded, the results suggest that ovarian and other genitourinary development is variably impaired in XX patients with distal 9p monosomy.

Ovarian and other genitourinary phenotype has been reported in a total of seven karyotypic female patients with molecularly defined distal 9p monosomy (Table 1) (this report and [2–5]). Ovarian function is highly variable, including overt primary hypogonadism in cases 1 and 3, borderline hypergonadotropinism in case 4, normal histological findings in case 6, positive menses in cases 2 and 5, and proven fertility in case 7. Such diverse ovarian development in XX patients is consistent with the presence of a gene(s) involved in the development of indifferent gonad common to both sexes or subsequent ovarian differentiation specific to females. Furthermore, external genital, anoperineal, and renal abnormalities are exhibited by some of the seven cases. This would suggest the presence of a gene(s) for genitourinary development on distal 9p. In support of this, external genital and anoperineal lesions have often been described in XX patients with distal 9p deletions, and renal lesions have occasionally been reported in XX and XY patients with distal 9p deletions, although molecular studies have not been performed in such patients [17–20].

The deletion maps of the seven cases are shown in Fig. 2, together with the karyotypes. Several points should be made with respect to genoype-phenotype correlations. First, haploinsufficiency of genes involved in human development is usually associated with a wide range of penetrance and expressivity, probably depending on other genetic and environmental factors [21]. Indeed, male sex development is highly variable in XY patients with distal 9p monosomy [3,17]. Second, as indicated by the development of renal dysfunction from ~6 years of age in case 2, several features could be age-dependent, so that they may be unrecognized if not assessed at an appropriate age. Third, some features such as renal lesion would be overlooked without appropriate examinations. These points imply that the absence of a specific feature does not warrant the preservation of a relevant gene, while the presence of a specific feature indicates loss of a relevant gene.

Thus, deletion mapping should primarily be based on the results in patients with clinically discernible phenotype. In this context, the gene(s) for ovarian development as well as that for anoperineal and renal development would be located to a roughly 11 Mb region distal to *D9S168*, and that for external genitalia development to an approximately 16 Mb distal to *D9S285*, on the basis of ovarian dysfunction in cases 1 and 3, external genital abnormality in cases 1 and 5, anoperineal lesion in cases 1–3, and renal lesion in cases 1 and 2 (Table 1). Lack of abnormal phenotype in cases

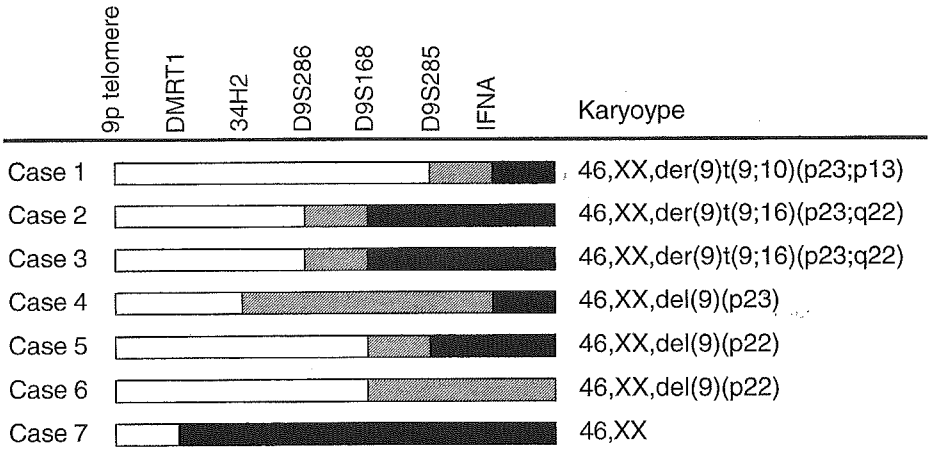

Fig. 2. Deletion maps and karyotypes of the seven patients with molecularly defined distal 9p monosomy. The case numbers correspond to those in Table 1. Of multiple loci examined in each case, the loci defining the breakpoint only are shown. The white and the black areas denote the monosomic and the disomic regions, respectively, and the striped areas depict the dosage unknown regions where the breakpoints should exist. According to the Ensembl Genome Browser at the Sanger Institute (http://www.ensembl.org/), the physical distance from the 9p telomere is roughly ~0.75 Mb for *DMRT1*, ~2.8 Mb for *34H2* (*D9S1136*), ~8.0 Mb for *D9S286*, ~10.6 Mb for *D9S168*, ~16.0 Mb for *D9S285*, and ~21 Mb for *IFNA*.

missing the critical regions would be explained by assuming incomplete penetrance. In particular, since the extent of ovarian and other genitourinary development is obviously different in related cases 2 and 3 who should have the identical size of 9p deletion, this argues for a wide range of penetrance. It may be possible, however, that another gene(s) for ovarian development or fertility and that for other genitourinary development reside in the more proximal region. Furthermore, it remains to be determined whether the gene(s) for ovarian development and that for other genitourinary development is identical or different, as is the gene(s) for ovarian development and that for testicular development.

Of multiple genes mapped on the critical regions defined in this study, *KANK* (kidney ankyrin repeat-containing protein) and *DMRT2* (doublesex and mab-3 related transcription factor 2) may be noteworthy. *KANK* is present at the position ~500 kb from the 9p telomere (distal to *DMRT1*) and is strongly expressed in the ovary [22], and *DMRT2* is present at the position ~1000 kb from the 9p telomere (proximal to *DMRT1*) and is strongly expressed in the kidney [23,24]. Thus, while detailed studies have not been performed, *KANK* and *DMRT2* could be regarded as candidate genes for ovarian and renal development, respectively. Although *Dmrt1*, a murine homolog for *DMRT1*, is expressed in the developing indifferent gonad [25], *DMRT1* is unlikely to be relevant to ovarian development: *Dmrt1* is most strongly expressed in the male-specific developing testis [25], and *Dmrt1* knockout XX mice have normal ovary, though *Dmrt1* knockout XY mice have defective testis development [26]. In addition, although the distal 9p region harbors *OVC* (ovarian adenocarcinoma oncogene), *OVC* is assigned between *IFNA* and *D9S169* and, therefore, maps outside the critical region defined in this study [27].

Cases 1–6 had a constellation of minor anomalies consistent with 9p monosomy syndrome [17]. In this regard, the critical region for 9p monosomy syndrome has been postulated between *D9S168* and *D9S144* by Veitia et al. [28] and between *D9S285* and *D9S286* by Christ et al. [29] (the locus order: 9p telomere–*D9S286*–*D9S144*–*D9S168*–*D9S285*–9p centromere), while the precise interval of the critical region and the number of relevant genes remain to be clarified. The 9p monosomy syndrome phenotype in cases 1–6 would primarily be compatible with the previously suggested location of the critical region for 9p monosomy syndrome.

In summary, the present study suggests that distal 9p monosomy results in not only variable degrees of impaired testicular development, but also diverse extent of defective ovarian and other genitourinary development. However, this notion remains speculative at present especially with regard to ovarian development, because the assessment of ovarian dysfunction in cases 1 and 3 is based on endocrine data only. Further studies will serve to define ovarian and other genitourinary phenotype in distal 9p monosomy, and to isolate the relevant gene(s).

Acknowledgments

This work was supported by a grant for Child Health and Development from the Ministry of Health, Labor, and Welfare (14C-1), and by a Grant-in-Aid from the Ministry of Education, Science, Sports, and Culture (15591150).

References

[1] C. Ottolenghi, K. McElreavey, Deletion of 9p and the quest for a conserved mechanism of sex determination, Mol. Genet. Metab. 71 (2000) 397–404.

[2] V. Calvari, V. Bertini, A. De Grandi, G. Peverali, O. Zuffardi, M. Ferguson-Smith, J. Knudtzon, G. Camerino, G. Borsani, S. Guioli, A new submicroscopic deletion that refines the 9p region for sex reversal, Genomics 65 (2000) 203–212.

[3] K. Muroya, T. Okuyama, K. Goishi, Y. Ogiso, S. Fukuda, J Kameyama, H. Sato, Y. Suzuki, H. Terasaki, H. Gomyo, K. Wakui, Y. Fukushima, T. Ogata, Sex determining gene(s) on distal 9p: clinical and molecular studies in six cases, J. Clin. Endocrinol. Metab. 85 (2000) 3094–3100.

[4] T. Ogata, K. Muroya, H. Ohashi, H. Mochizuki, T. Hasegawa, M. Kaji, Female gonadal development in XX patients with distal 9p monosomy, Eur. J. Endocrinol. 145 (2001) 613–617.

[5] E. Vialard, C. Ottolenghi, M. Gonzales, A. Choiset, S. Girard, J.P. Siffroi, K. McElreavey, C. Vibert-Guigue, M. Sebaoun, N. Joye, M.F. Portnoi, F. Jaubert, M. Fellous, Deletion of 9p associated with gonadal dysfunction in 46, XY but not in 46, XX human fetuses, J. Med. Genet. 39 (2002) 514–518.

[6] Japan Public Health Association, Normal biochemical values in Japanese children, Sanko Press, Tokyo, 1996 (in Japanese).

[7] J. Ito, T. Tanaka, R. Horikawa, Y. Okada, S. Morita, M. Koitaji, A. Tanae, I. Hibi, Serum LH and FSH levels during GnRH tests and sleep in children, J. Jpn. Pediatr. Soc. 97 (1993) 1789–1796, in Japanese.

[8] N. Matsuo, Skeletal and sexual maturation in Japanese children, Clin. Pediatr. Endocrinol. 2 (Suppl.) (1993) 1–4.

[9] B.K. Han, D.S. Babcock, Sonographic measurements and appearance of normal kidneys in children, AJR 145 (1985) 611–616.

[10] W.L. Flejter, J. Fergestad, J. Gorski, T. Varvilli, S. Chandrasekharappa, A gene involved in XY sex reversal is located on chromosome 9, distal to marker D9S1779, Am. J. Hum. Genet. 63 (1998) 794–802.

[11] Y. Ning, A. Roschke, A.C.M. Smith, M. Macha, K. Precht, H. Riethman, D.H. Ledbetter, J. Flint, S. Horsley, R. Regan, L. Kearney, S. Knight, K. Kvaloy, W.R.A. Brown, A complete set of human telomeric probes and their clinical application, Nat. Genet. 14 (1996) 86–89.

[12] S.J.L. Knight, C.M. Lese, K.S. Precht, J. Kuc, Y. Ning, S. Lucas, R. Regan, M. Brenan, A. Nicod, N.M. Lawrie, D.L. Cardy, H.T.J. Nguyen, H.C. Riethman, D.H. Ledbetter, J. Flint, An optimized set of human telomere clones for studying telomere integrity and architecture, Am. J. Hum. Genet. 67 (2000) 320–332.

[13] M. Bouzyk, S.P. Bryant, C. Evans, S. Guioli, S. Ford, K. Schmidt, P.N. Goodfellow, S. Povey, M. Rebello, S. Rousseaux, N.K. Spurr, Integrated radiation hybrid and yeast artificial chromosome map of chromosome 9p, Eur. J. Hum. Genet. 5 (1997) 299–307.

[14] S. Povey, J. Attwood, B. Chadwick, J. Frezal, J.L. Hains, M. Knowles, D.J. Kwiatkowski, O.I. Olopade, S. Slaugenhaupt, N.K. Spurr, M. Smith, K. Steel, J.A. White, M.A. Pericak-Vance, Report of the fifth international workshop on chromosome 9, Ann. Hum. Genet. 61 (1997) 183–206.

[15] R. Illig, M. Tolksdorf, G. Mürset, A. Prader, LH and FSH response to synthetic LH-RH in children and adolescents with Turner's and Klinefelter's syndrome, Helv. Paediatr. Acta 30 (1975) 221–231.

[16] J.L. Ross, D.L. Loriaux, G.B. Cutter Jr., Developmental changes in neuroendocrine regulation of gonadotropin secretion in gonadal dysgenesis, J. Clin. Endocrinol. Metab. 57 (1983) 288–293.

[17] J.L. Huret, C. Leonard, B. Forestier, M.O. Rethoré, J. Lejeune, Eleven new cases of del (9p) and features from 80 cases, J. Med. Genet. 25 (1988) 741–749.

[18] V. Shashi, W.L. Golden, J.S. Fryburg, Choanal atresia in a patient with the deletion (9p) syndrome, Am. J. Med. Genet. 49 (1994) 88–90.

[19] R. Ion, L. Telvi, J.L. Chaussain, J.P. Barbet, M. Nunes, A. Safar, M.O. Rethore, M. Fellous, K. McElreavey, Failure of testicular development associated with a rearrangement of 9p24.1 proximal to the SNF2 gene, Hum. Genet. 102 (1998) 151–156.

[20] R.A. Pfeiffer, A. Rauch, U. Trautmann, H.G. Dorr, O. Hiort, G. Scherer, G. Rosch, T. Papadopoulos, K. Hardt, E. Lachmann, Defective sexual development in an infant with 46,XY,der (9)t (8;9) (q23.1;p23)mat, Eur. J. Pediatr. 158 (1999) 213–216.

[21] E. Fisher, P. Scambler, Human haploinsufficiency: one for sorrow, two for joy, Nat. Genet. 7 (1994) 5–7.

[22] T. Nagase, N. Seki, K. Ishikawa, A. Tanaka, N. Nomura, Prediction of the coding sequences of unidentified human genes. V. The coding sequences of 40 new genes (KIAA0161-KIAA0200) deduced by analysis of cDNA clones from human cell line KG-1, DNA Res. 29 (1996) 17–24.

[23] C. Ottolenghi, R. Veitia, L. Quintana-MurcL, D. Torchard, L. Scapoli, N. Souleyreau-Therville, J. Beckmann, M. Fellous, K. McElreavey, The region on 9p associated with 46, XY sex reversal contains several transcripts expressed in the urogenital system and a novel doublesex-related domain, Genomics 64 (2000) 170–178.

[24] C. Ottolenghi, R. Veitia, M. Barbieri, M. Fellous, K. McElreavey, The human doublesex-related gene, DMRT2, is homologous to a gene involved in somitogenesis and encodes a potential bicistronic transcript, Genomics 64 (2000) 179–186.

[25] C.S. Raymond, J.R. Kettlewell, B. Hirsch, V.J. Bardwell, D. Zarkower, Expression of Dmrt1 in the genital ridge of mouse and chicken embryos suggests a role in vertebrate sexual development, Dev. Biol. 215 (1999) 208–220.

[26] C.S. Raymond, M.W. Murphy, M.G. O'Sullivan, V.J. Bardwell, D. Zarkower, Dmrt1, a gene related to worm and fly sexual regulators, is required for mammalian testis differentiation, Genes Dev. 14 (2000) 2587–2595.

[27] G. Chenevix-Trench, J. Kerr, M. Friedlander, T. Hurst, B. Sanderson, M. Coglan, B. Ward, J. Leary, S.K. Khoo, Homozygous deletions on the short arm of chromosome 9 in ovarian adenocarcinoma cell lines and loss of heterozygosity in sporadic tumors, Am. J. Hum. Genet. 55 (1994) 143–149.

[28] R.A. Veitia, M. Nunes, L. Quintana-Murci, R. Rappaport, E. Thibaud, F. Jaubert, M. Fellous, K. McElreavey, J. Goncalves, M. Silva, J.C. Rodrigues, M. Caspurro, F. Boieiro, R. Marques, J. Lavinha, Swyer syndrome and 46, XY partial gonadal dysgenesis associated with 9p deletions in the absence of monosomy-9p syndrome, Am. J. Hum. Genet. 63 (1998) 901–905.

[29] L.A. Christ, C.A. Crowe, M.A. Micale, J.M. Conroy, S. Schwartz, Chromosome breakage hotspots and delineation of the critical region for the 9p-deletion syndrome, Am. J. Hum. Genet. 65 (1999) 1387–1395.